Contributions to Geophysics and Geodesy Vol. 47/3, 2017 (149–199)

The major tectonic boundaries of the Northern Red Sea rift, Egypt derived from geophysical data analysis

Salah SALEH[1], Oya PAMUKÇU[2], Ladislav BRIMICH[3]

[1] National Research Institute of Astronomy and Geophysics (NRIAG), 11421 Helwan, Cairo, Egypt; e-mail: salahsmm@yahoo.com

[2] Department of Geophysics, Faculty of Engineering, Dokuz Eylul University, 35160 Buca, Izmir, Turkey; e-mail: oya.pamukcu@deu.edu.tr

[3] Earth Science Institute of the Slovak Academy of Sciences, Dúbravská cesta 9, 840 05 Bratislava, Slovak Republic; e-mail: geofbrim@savba.sk

Abstract: In the present study, we have attempted to map the plate boundary between Arabia and Africa at the Northern Red Sea rift region including the Suez rift, Gulf of Aqaba-Dead Sea transform and southeastern Mediterranean region by using gravity data analysis. In the boundary analysis method which was used; low-pass filtered gravity anomalies of the Northern Red Sea rift region were computed. Different crustal types and thicknesses, sediment thicknesses and different heat flow anomalies were evaluated. According to the results, there are six subzones (crustal blocks) separated from each other by tectonic plate boundaries and/or lineaments. It seems that these tectonic boundaries reveal complex structural lineaments, which are mostly influenced by a predominant set of NNW–SSE to NW–SE trending lineaments bordering the Red Sea and Suez rift regions. On the other side, the E–W and N–S to NNE–SSW trended lineaments bordering the South-eastern Mediterranean, Northern Sinai and Aqaba-Dead Sea transform regions, respectively. The analysis of the low pass filtered Bouguer anomaly maps reveals that the positive regional anomaly over both the Red Sea rift and South-eastern Mediterranean basin subzones are considered to be caused by the high density of the oceanic crust and/or the anomalous upper mantle structures beneath these regions whereas, the broad medium anomalies along the western half of Central Sinai with the Suez rift and the Eastern Desert subzones are attributed to low-density sediments of the Suez rift and/or the thick upper continental crustal thickness below these zones. There are observable negative anomalies over the Northern Arabia subzone, particularly in the areas covered by Cenozoic volcanics. These negative anomalies may be attributed to both the low densities of the surface volcanics and/or to a very thick upper continental crust. On the contrary, the negative anomaly which belongs to the Gulf of Aqaba-Dead Sea transform zone is due to crustal thickening (with limited heat flow values) below this region. Additionally in this study, the crustal thinning was investigated with heat flow, magnetic and free air gravity anomalies in the Northern Red Sea rift region. In fact, the crustal thinning of the study area was also proportional to the regions of observable high heat flow values. Finally, our

doi: 10.1515/congeo-2017-0010

results were found to be well correlated with the topography, free air, aeromagnetic and heat flow dataset profiles crossing most of the study area.

Key words: Red Sea rift, potential field, low pass filtering, boundary analysis, crustal structure

1. Introduction

The Red Sea was formed by extensional rupturing of the Precambrian lithosphere beginning in the Late Oligocene. Sea floor spreading began about 5 Ma in the southern Red Sea (*Roeser, 1975*) and the transition from continental to oceanic rifting is occurring today in the Central and Northern Red Sea (*Martinez and Cochran, 1988; Guennoc et al., 1990; Cochran et al., 1991*).

Based on the geophysical data in the Northern Red Sea, *Cochran (2005)* suggested that rift development occurs via the rotation of large crustal fault blocks that sole into a zone of plastic creep in the lower crust, resulting in a flat Moho and high upper crustal relief. Initial broadly distributed extension is eventually replaced by focused extension at the rift axis leading to rapid lithospheric thinning and melt generation. Melt formed within individual rift segments is focused to form small axial volcanoes (*Cochran 2005*).

This study is focused on the northern Red Sea rift from 25° to 28° N (Fig. 1), where small cells of magmatic extension are just beginning to nucleate at the axis of what has been nearly magmatic rift (*Cochran and Karner, 2007*). The purpose of this paper is to utilize a new compilation and synthesis of geophysical data from the northern Red Sea to map the plate boundary around and in this continental Rift.

We used the Boundary Analysis method (*Cordell and Grauch, 1982, 1985; Blakely and Simpson, 1986*) to identify boundaries of gravity contacts by calculating the horizontal gradient magnitudes of the gridded gravity anomaly data. The method has been used by several previous studies (*Ekinci and Yiğitbaş, 2012, 2015*).

In this study, first of all, different types of filters were applied to Bouguer gravity values for the study area, and then the boundary analysis method was applied. The horizontal gradient amplitudes were calculated from the Bouguer gravity anomaly on space domain and then the location of the

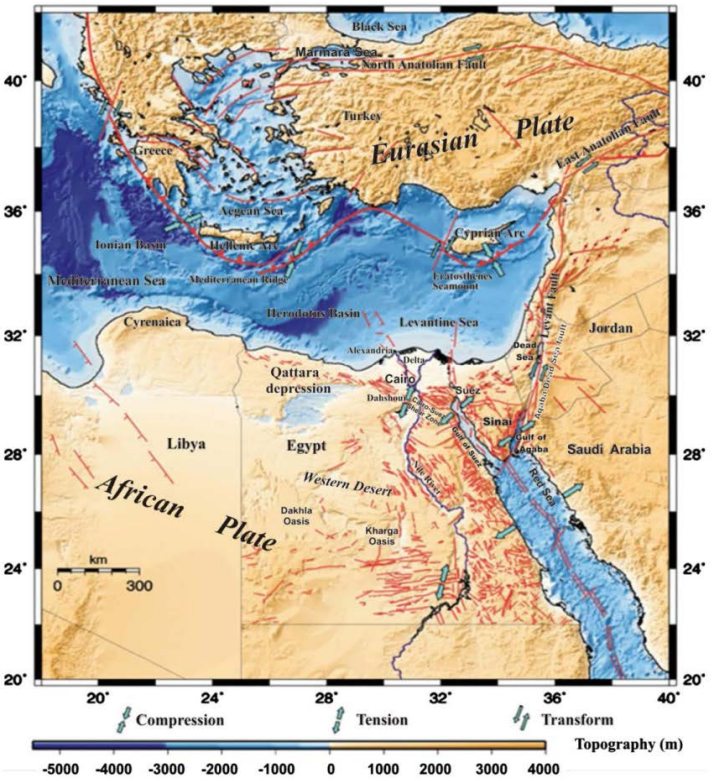

Fig. 1. Tectonic boundaries of the Eastern Mediterranean Region. Red lines delineate recent surface faults, Red Sea Axial rift, and tectonic boundaries (compiled after *Abou Elenean, 2007* – for interpretation of the references in this figure legend, the reader is referred to the web version of this article).

horizontal gradients were computed, and finally a new plate boundary map was constrained. According to these results, six subzones (crustal blocks) are estimated and separated from each other by tectonic plate boundaries.

Finally, crustal thinning for the northern Red Sea rift region was also discussed. Thin crustal zone values were remarked in a region where magnetization decreased while the amplitude of the free air anomalies increased (*Von Frese et al., 1982; Pamukçu et al., 2007*). Comparing the same previous approach with heat flow anomaly values, we can conclude that, the crustal thinning of the study area was also nearly noteworthy beneath regions of very high heat flow values (*Saleh et al., 2013*).

2. Tectonic and geological settings

Egypt is located in the north-eastern corner of the African continent and is bounded by three active tectonic margins: the African Eurasian plate margin; the Red Sea plate margin; and the Aqaba-Dead Sea fault (Fig. 1). This in turn creates critical continental conditions that are responsible for the major seismic activities in Egypt since prehistoric time. The recent geodetic data and GPS measurements imply that the African plate is moving NW with respect to Eurasia with a velocity of 6 mm/year (*McClusky et al., 2000*) and the spreading rates along the Red Sea decrease from 14 mm/year at 15° N to 5.6 mm/year at 27° N. Along the southernmost segment of the Aqaba-Dead Sea fault, motion is a left-lateral strike-slip of 5.6 mm/year (*McClusky et al., 2003*). This left-lateral motion shows a rate of about 2.8 mm/year in the northern segment of the Dead Sea with slight spreading of the Suez rift (*Wdowinski et al., 2004*).

This yields some secondary deformation manifested by moderate earthquake activity along the northern Egyptian coast. Based on geophysical studies in the territory of Egypt, three major tectonic trends are recognized, namely the Red Sea trend oriented NW–SE, the Gulf of Aqaba trend oriented NE–SW and the Mediterranean trend oriented E–W (*Yousef, 1968*). Owing to these complex tectonics, the distribution of seismic activity in Egypt is observed in four narrow belts: Levant–Aqaba; Northern Red Sea–Gulf of Suez–Cairo–Alexandria; Eastern Mediterranean–Cairo–Fayum; and the Mediterranean Coastal Dislocation (*Sieberg, 1932; Ismail, 1960; Maamoun et al., 1984; Kebeasy, 1990; Abou Elenean, 1997*).

The north-eastern part of Egypt is dominated by the relative movements of major plates (Africa, Arabia and Eurasia) and relatively aseismic small plates. The Red Sea, which forms the boundary between the African plate and the Arabian plate, bifurcates into two branches: the Gulf of Suez and the Gulf of Aqaba. The Gulf of Suez follows the main trend of the Red Sea and constitutes the boundary between the African plate and the Sinai subplate (*Said, 1963; Youssef, 1968*). The Suez Rift is considered to be the plate boundary between the African and Sinai Subplates (*McKenzie et al., 1970; Le Pichon and Francheteau, 1978*). In general, it is accepted that the Gulf of Suez and Red Sea depressions were formed by the anti-clockwise rotation of the Arabian Plate away from the African Plate (*Cochran, 1983*).

Several geological and seismological investigations assert that the area surrounding the Gulf of Suez displayed, in the past, extensional tectonics with a large deformation rate (e.g., *Ben-Menahem et al., 1976; Le Pichon and Gaulier, 1988; Steckler et al., 1988, 1998; Piersanti et al., 2001*). The tectonics of the Sinai Peninsula and the Gulf of Aqaba is strongly dominated by the active boundaries between the African and the Arabian plates (Fig. 1) that are separated from each other. According to the current literature, from the Neogene to Late Miocene, this area was subjected to different phases of motion.

Geologically, the oldest known formation in the study area is of Late Precambrian age, igneous and metamorphic rocks form the northern edge of the African Shield (Fig. 2). *Saleh et al. (2006)* evaluated outcropping

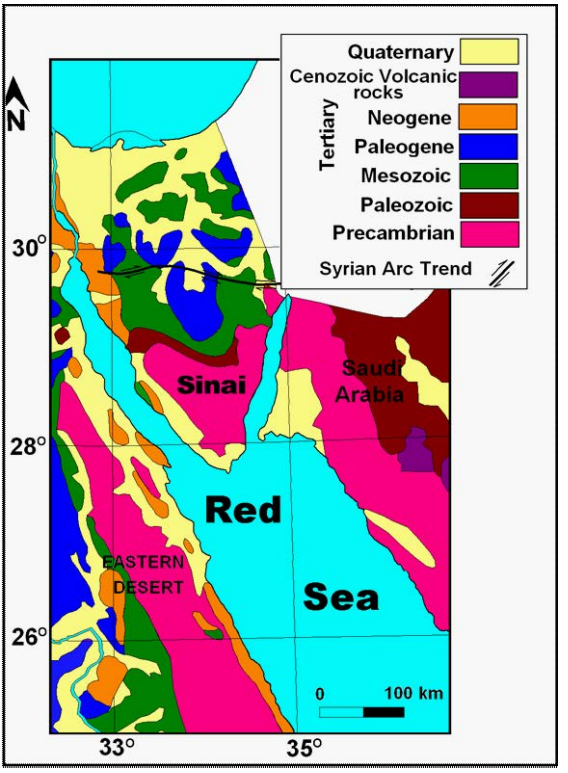

Fig. 2. Geological map of Northern Egypt and its surroundings (modified after *U.S. Geological Survey, 1963; Neev, 1975; EGSMA, 1993*).

of the basement complex in southern Sinai and in the Eastern Desert (Red Sea mountain range) using 3D Geophysical modelling. *Said (1962), El-Geziry and Marzouk (1974), Saleh et al. (2013)* showed that the depth to the basement increases going north towards the Mediterranean Sea.

Generally the Egyptian platform may be subdivided into four major structural domains (e.g., *Said, 1962; Meshref, 1990*) with one minor one, as seen in Fig. 3. The study area covers all of them, namely:

1) **The Nerubian-Arabian Shield (Craton)**, the shield is well exposed in the Sinai Peninsula, the Eastern desert and in the extreme southern part of the Western Desert. It consists essentially of Precambrian rocks. *El Shazly (1977)* distinguishes several stages within these metamorphic sequences of geosynclinals Archean formations with frequent intrusion of plutonic and volcanic rocks.

2) **The Stable Shelf**, the shelf embraces the area north and west of the Nerubian-Arabian shield. It exhibits a gentle tectonic deformation and its sedimentary cover is mainly represented by continental and epicontinental deposits such as the Mesozoic Nubian Sandstone. The Sedimentary sequence on the stable shelf is relatively thin with some 400 metres of sediment near the Nerubian-Arabian area and increasing to as much as 2500 metres near the transition into the unstable shelf to the north. It is composed of sand and shale in its lower section and of shallow water carbonates in its upper part.

3) **The Unstable Shelf** is situated north of the stable shelf with the transition between two structural-depositional units following a line approximately set from the Siwa Oasis through the Farafra Oasis and Suez into Central Sinai. The sedimentary sequence of the unstable shelf is relatively thick with the lower part of the section composed mainly of clastic sediment, followed up section by a middle calcareous series and topped by a blanket of biogenic carbonates. The formation is gently folded and shows sign of lateral stress. Overthrust by the northern structure is reported. This structural deformation is related to the Laramide phase of the Alpine Orogeny. The trends of this fold bundle are lightly trended to the north-east and referred to as The Syrian Arc system.
   The Gulf of Suez–Red Sea Graben is a subsidence area within the stable shelf and the northern part of the Nerubian-Arabian shield. It was

formed originally during Palaeozoic times as a narrow embayment of Tethys and intensively rejuvenated during the rifting phase of the great East Africa Rift system in Lower to Middle Tertiary times. Great accumulation of sediments form this fast subsiding depression, interrupted occasionally by general and regional uplift with subsequent erosion. It is connected to the Mediterranean Sea to the north and Red Sea to the south, it was established during the Early Miocene as witnessed by the distribution of Mediterranean fauna from the north as far south as the southern Red Sea. The Red Sea originated during the Oligocene time after the arching and crustal thinning in the general area of the Nerubian-Arabian Shield and the subsequent collapse, in the context of East African rifting. Spreading of the Red Sea floor was and still relates to the relative motion of various plates present in north-eastern Africa and the Near East.

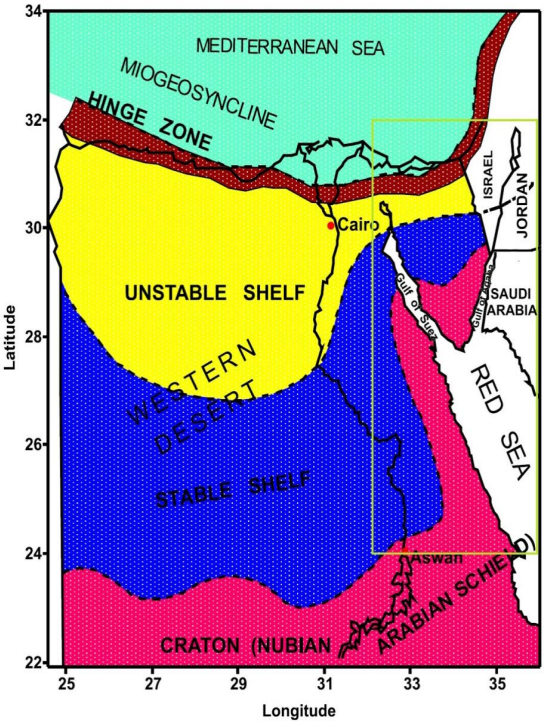

Fig. 3. The main geographical features and major tectonic trends of Egypt (after *Meshref, 1990*). The study area is also shown (green framed area).

4) **The Hinge Zone**, located between the mobile shelf and the miogeosynclinal basinal area; it is characterized by a rapid thickening of Oligocene to Pliocene sediments, and partially coincides with the present Mediterranean coastal area.

5) **The Miogeosyncline**, now partially buried under thick Plio-Pleistocene deposits of the Nile Delta; the structural grain of the basement is dominated by two orthogonal trends induced by successive diastrophic phases; the sedimentary formations are gently folded and over thrusting is also locally reported; the described deformation is related to the Laramide phase of the Alpine orogeny; the trend of these folds is lightly arcuate to the north-east and referred to as the Syrian Arc.

3. Applications

3.1. Bouguer datasets of the Northern Red Sea Rift

3.1.1. Bouguer data source

Considerable amounts of gravity data are now available to unravel the gross crustal structure of Egypt. The Bouguer anomaly map of our study area (Northern Red Sea and south-eastern Mediterranean), at a constant contour interval of 5 mGal (Fig. 4), has been regridded by the World Gravity Map project team (WGM), from various published maps (*Allan and Morelli, 1970; Riad, 1977; Woodside, 1976, 1977; Egyptian General Petroleum Corporation (EGPC), 1990; Folkman and Assael, 1980; Ben-Avraham, 1985; Tealeb and Riad, 1986; Minich, 1987; Martinez and Cochran, 1988; Kamel, 1990; Ginzburg et al., 1993; Makris and Wang 1994; Rybakov et al., 1997; Segev et al., 2006*).

Marine gravity data in the northern Red Sea were taken from publications (*Minich, 1987; Martinez and Cochran, 1988*), whereas in South-eastern Mediterranean were taken from previous literature (*Woodside 1976, 1977; Ginzburg et al., 1993; Makris and Wang, 1994*). In addition to this, Sinai Peninsula data were collected from *Tealeb and Riad (1986)*. A complete file of the datasets is available now on a web site at: `http://bgi.omp.obs-mip.fr/index.php/eng/Activities/Projects/World-Gravity-Map-WGM`.

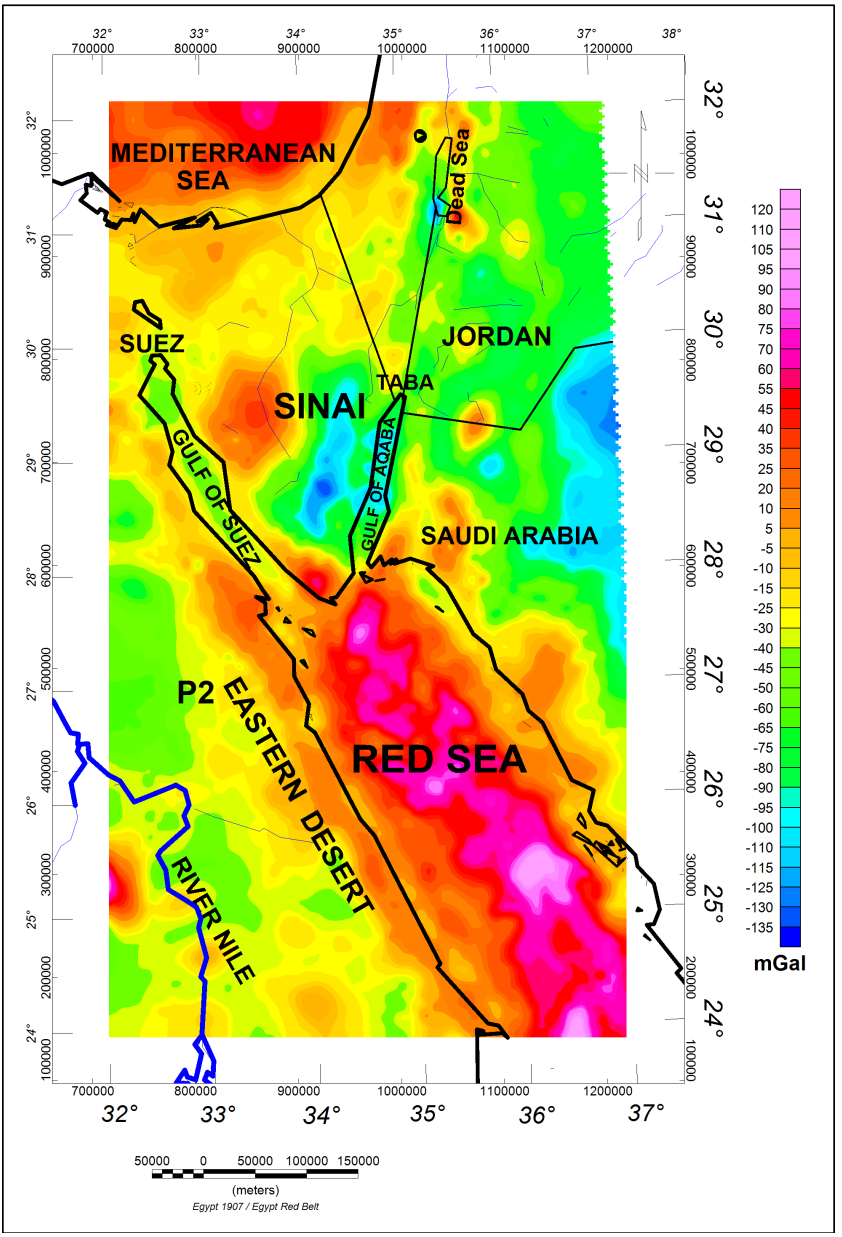

Fig. 4. Bouguer gravity anomaly of the Northern Red Sea Rift region.

3.1.2. Correction of Gravity data

The distance between the consecutive observation stations ranges approximately from 2 to 5 km. The calculated Bouguer gravity anomaly is based on the international gravity formula of 1967, referenced to the IGSN-1971, reduced to sea level and corrected with the standard density of reduction, 2670 kg/m^3. For onshore stations, terrain corrections up to 50 m were made in the field using topographic charts and Hammer tables (*Hammer, 1939*). The horizontal positions of the stations were obtained from 1:500,000 topographic sheets. The station locations were converted to the Universal Transverse grid coordinates with the central Meridian at 30° E. Elevations at each station were measured by a barometric altimeter and all measurements were referenced to absolute elevation. The corrections were applied to all the land stations which were discussed in more detail previously by *Kamel (1990)*.

3.1.3. Interpretation of Bouguer anomalies

The general trend of the Bouguer gravity anomalies is NW–SE. At the southern tip of the Sinai Peninsula, the gravity field switches from positive to negative values in the Gulfs of Suez and Aqaba. Both the Gulfs of Suez and Aqaba are characterized by gravity minima with the values in the Gulf of Suez approximately one-half those found in the Gulf of Aqaba. Along the Dead Sea Rift itself the Bouguer anomaly field is characterized by very steep gradients towards the Rift Zone and a series of strong negative gravity closures from north to south. The anomaly increases in magnitude with a decrease in the relief of the topography and attains its maximum of +95 mGal along the axis of the Red Sea rift floor. A slight systematic decrease of the amplitude occurs towards the north; where the maximum amplitude is of the order 80 mGal in the southern part of Gulf of Aqaba. The highest mountains in the Red Sea margins, for example, have values of over 1000 m, and their negative Bouguer anomalies are only about −10 to −30 mGal, aligned parallel to the Red Sea along a NNW trend. Alternative negative and positive anomalies along the Gulf of Suez may be due to the faulted blocks or presence of different basins with different thickness of sedimentary sequence in the area. This leads to the conclusion that the shallow parts are extending along the two Gulfs and southern part of Sinai

where the basement rocks outcrop (Fig. 3). An elongated anomaly was observed with gravity value between −35 and −50 mGals extending from 26° to 28.5° N and 31.5° to 33° E. The elevation of this area is fairly smooth and only 200 to 400 m above sea level. The Red Sea Mountains with altitudes over 800 m show Bouguer anomalies between −10 mGals and −35 mGals, the values increasing to zero gravity level at the Red Sea coast. These anomalies suggest that the crust attains its maximum thickness below the Red Sea Mountains and gets considerably thinner towards the Red Sea Rift (*Saleh et al., 2006*). In the Red Sea, the anomalies are positive; the anomaly increases in magnitude with a decrease in the relief of the topography and attains its maximum of +80 mGal along the axis of the Red Sea Rift floor. In eastern Egypt and the Gulf of Suez, the anomalies have a NNW–SSE trend which is associated with the Miocene and Post Miocene opening of the Red Sea and Gulf of Suez.

3.1.4. Bouguer data analysis

In the first stage of the study, the low passed filtered technique with different frequency domains were applied to analyse the Bouguer anomaly dataset. To find the impact of the deepest structure, the low passed filtered parameters were estimated as the cutting frequency; $fc = 0.01$ km^{-1} and filter dimension; 11×11 (Fig. 5). The filtered Bouguer gravity anomaly map (Fig. 5) was used to enhance the anomaly wave length associated with deep sources. This map reveals the influence of the regional gravity field and demonstrates a general smooth trend pattern. The most attractive feature of this map is that, it readily shows alternating high and low linear and isometric anomalies of the NW–SE trend occupying Saudi Arabia, the Red Sea and Suez rift regions. On the other side, the E–W and N–S to NNE–SSW trending anomalies are in the south-eastern Mediterranean, northern Sinai and Aqaba-Dead Sea transform regions, respectively. Then, we used filtered Bouguer gravity values as in Fig. 5 (Appendix I) and the boundary locations were obtained as in Fig. 6.

The approach of *Von Frese et al. (1982)* which has been used as an investigation basis of inversely proportional correlation between long wavelength, was applied to free air gravity and low magnetic data. *Von Frese et al. (1982)* pointed out that a thin crust was observed in a region where mag-

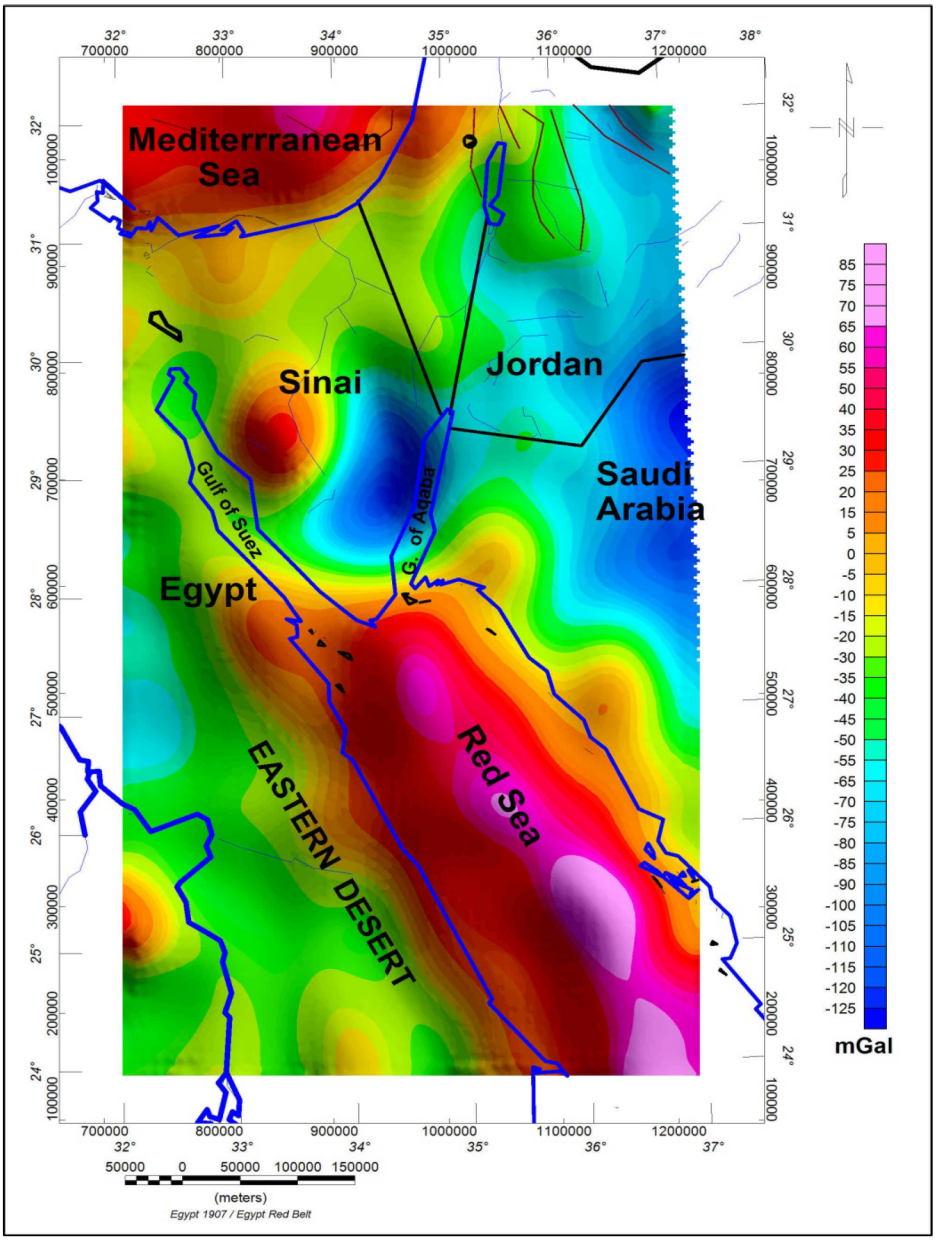

Fig. 5. Filtered Bouguer anomaly map (map grid interval 0.1 data set 49×81).

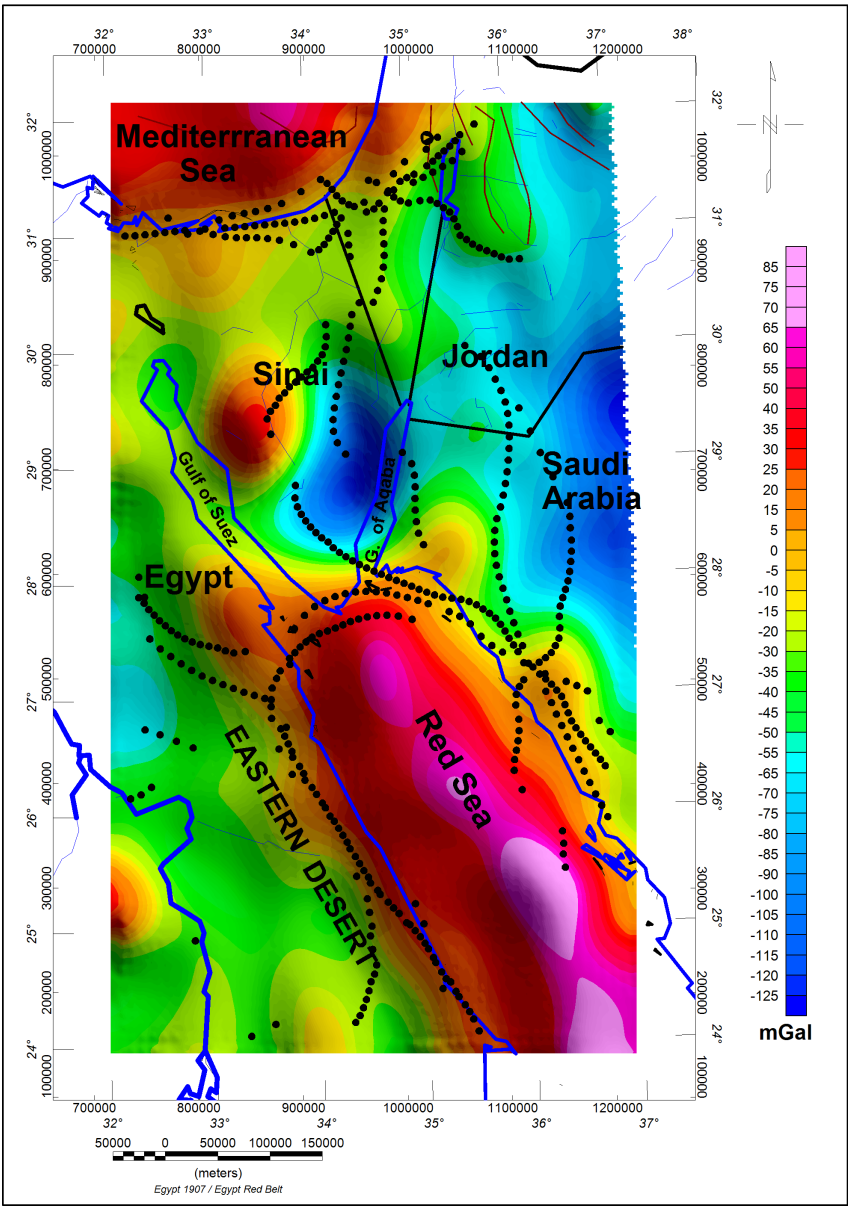

Fig. 6. Filtered Bouguer anomaly map (map grid interval 0.1 data set 49 × 81) with boundary analysis (black point).

netization decreased but the amplitude of the free air anomalies increased. Using the same approach, crustal thickness was estimated by determining the areas (*Pamukçu et al., 2007*). The magnetic anomaly with decreasing amplitude being inversely proportional to the free air gravity anomaly is seen together with high heats together with iso-statistically unbalanced altitudes, and with various geodynamic processes that result in depleted crust and mantle intrusions. Following the application of filtering and horizontal gradient techniques to Bouguer gravity data, the results can be associated with differences in crustal thickness, heat flow, seismic activity, basement surface (sedimentary thickness) and fault structures. However, like any potential field model which is ambiguous, we sought to constrain the tectonic boundary by integrated interpretation of available free air, magnetic and topographic data analysis.

3.2. Magnetic datasets of Northern Red Sea rift

The study region includes land, marine and magnetic surveys for the northern Red Sea rift region and its surroundings including the Gulf of Suez, Gulf of Aqaba, Sinai Peninsula, and northern parts of the Eastern Desert. The magnetic map, which includes the Sinai Peninsula and some regions of the eastern desert, was prepared by the *EGPC (1990)*, with a flight elevation of 1 km. The land magnetic survey was performed using two magnetic protons of geometric type. One instrument was used as a base station for diurnal corrections for each profile, and the second one was used to measure the observed magnetic data. The distance between the stations ranged from 200 to 300 m according to the changes in the recorded geomagnetic data. The marine magnetic map was compiled for both the Gulf of Suez and the northern Red Sea based on *Cochran et al. (1986)* and *Meshref (1990)*. The total magnetic intensity data resulting from different magnetic surveys was compiled and reduced to one set of data.

Recently, the magnetic data sets became available after compilation through the World Digital Magnetic Anomaly Map project; WDMAM: (`http://models.geomag.us/wdmam.html` and GETECH: `http://www.getech.com/`).

The magnetic fields due to geological bodies are distorted by the local inclination and declination of the Earth's magnetic field, making it difficult

to estimate their shapes and locations correctly. In order to eliminate that effect in the appearance of an anomaly, which depends on the magnetic latitude of the survey area as well as on the dip angle of the magnetization vector in the body, a mathematical procedure known as reduction to the pole (RTP) was applied to the grid of total magnetic intensity values using the geosoft program (*Geosoft, 2008*). The resultant map was then reduced to the north magnetic pole map (Fig. 7), which is more usable, because its anomalies are independent on the magnetic inclination of the source bodies. The RTP map shows the distribution and relief of the exposed basement rocks. High magnetic anomalies can be observed in the southern part of the Sinai Peninsula which well matches with the exposed geological units that are mainly composed of igneous rocks (back to the geological map in Fig. 2). The map also indicates that most of the observed anomalies show NE–SW, NW–SE and N–S trend patterns with some sharp gradients at varying locations. Since the magnetic maps are related directly to the basement rock features, this indicates the presence of a basement relief change. It is also possible to observe that the Sinai Peninsula is divided into two geological provinces based on the magnetic features. The southern province is characterized by high magnetic anomalies and the Northern Province with low magnetic anomalies.

In addition, the RTP map clarifies a pattern of magnetic anomalies within the marine portion of the northern Red Sea that exhibits a relatively flat magnetic field on which a number of large-amplitude dipolar anomalies are superimposed. Magnetic anomalies in the northern Red Sea are all dipolar anomalies (Fig. 7) implying a compact localized source. These anomalies have been interpreted as arising from discrete localized volcanoes (*Cochran et al., 1986; Martinez and Cochran, 1988*).

3.3. Topographic and Free Air gravity anomaly of the northern Red Sea region

In the north, the Red Sea bifurcates into the Gulfs of Suez and Aqaba. The floor of the Gulf of Suez is quite smooth and the depth of water is shallow, averaging about 55 m. In contrast, the Gulf of Aqaba has varied bottom topography with much greater depths of water reaching 1460 m. North of latitude 24° to 25° N, the Red Sea consists of one main trough

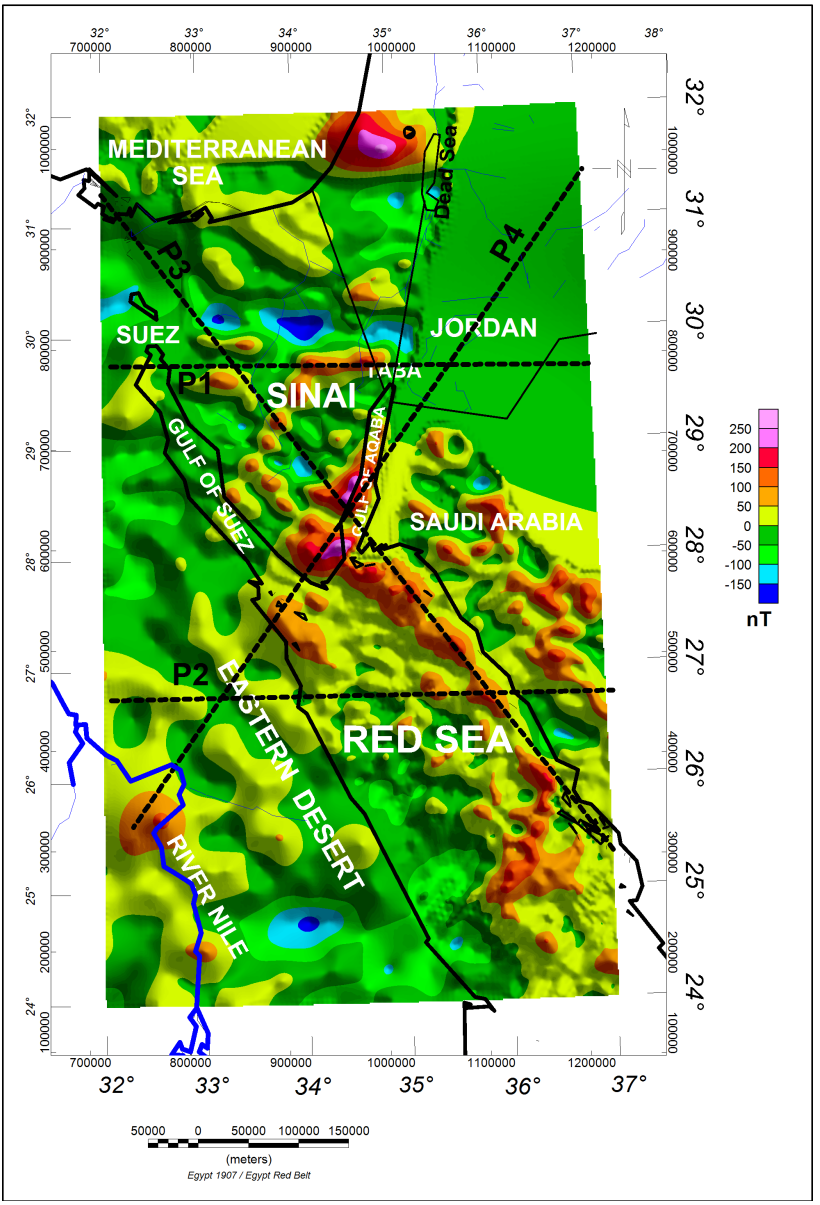

Fig. 7. Total magnetic anomaly map reduced to the pole of the Northern Red Sea Rift region. Contour interval is 50 nT. The locations of the sections of Figs. 14a–e are shown with black dashed lines.

approximately 150 km in width with shallow shelves on either side some 30 to 40 km in width (Figs. 1 and 8). The water depth in the trough is about 1000 m and the shorelines are straight.

The bathymetry of the active, main trough of the northern Red Sea rift, consists of a series of terraces stepping down to an axial depression at a depth of 1100–1200 m (*Martinez and Cochran, 1988; Cochran, 2005*). Sediment deformation within the axial depression is much more intense than in the remainder of the Red Sea (*Knott et al., 1966; Guennoc et al., 1988; Martinez and Cochran, 1988*), implying that tectonic activity and extension is presently concentrated predominantly in the axial depression.

Although earthquakes with $M_L = 3$ are also concentrated in the axial depression, smaller earthquakes are distributed throughout the northern Red Sea (*Badawy, 2005*). These two observations imply that some extension still occurs within the main trough away from the axial depression.

The satellite altimeter free air gravity anomaly of the northern Red Sea region is given in Fig. 9 as computed by *Sandwell and Smith (1997)*. The free air gravity anomaly map of the northern Red Sea is generally characterized by negative free air gravity anomalies with average values of about 0 to −20 mGal in the margin areas and a consistent gravity low from −30 to −40 mGal of the axial depression. A "Y" shaped region of very low values of a minimum −70 mGal is found near the junction of the Red Sea with the Suez and Aqaba Gulfs. A series of elongated gravity highs parallel to the overall Red Sea trend are located outside the axial rift. High gravity anomalies ranging from 0 to 20 occur on some seaward terraces. Moreover, a series of smaller structural features appears on both side of the axial rift of the Red Sea. These may be attributed to irregular bathymetry of the Red Sea (Fig. 8) related to the spreading along the axial Rift (*Martinez and Cochran, 1988*). Most of these small terraces coincide with bathymetric features especially the negative anomaly of the axial rift or the varying anomaly terraces along the axial rift as shown in Fig. 8.

4. Crustal structures, heat flow and seismicity

Several studies have been carried out to evaluate the crustal structure in the northern Red Sea, Egypt and Arabian Shield by using data observed from

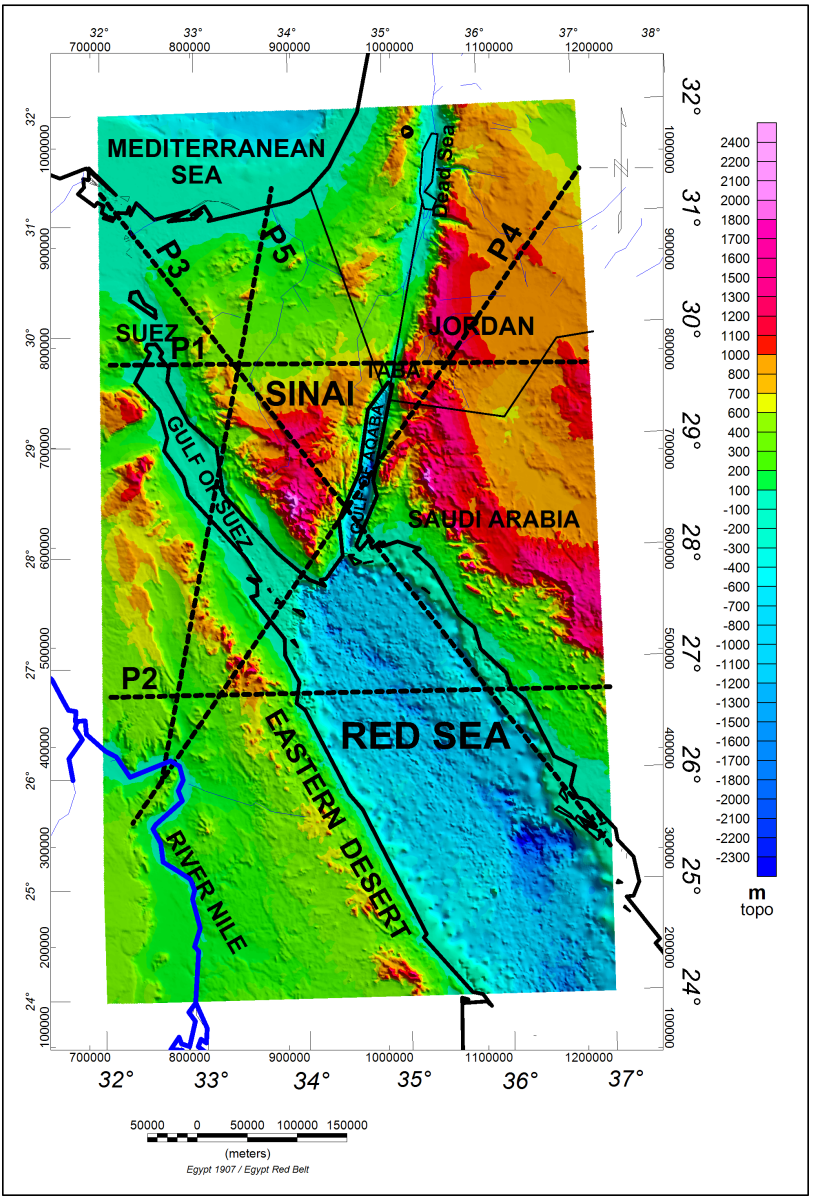

Fig. 8. Topographic and bathymetric anomaly map of the Northern Red Sea Rift region (derived from *Sandwell and Smith, 1997*). Locations of the sections of Figs. 14a–e are shown with black dashed lines.

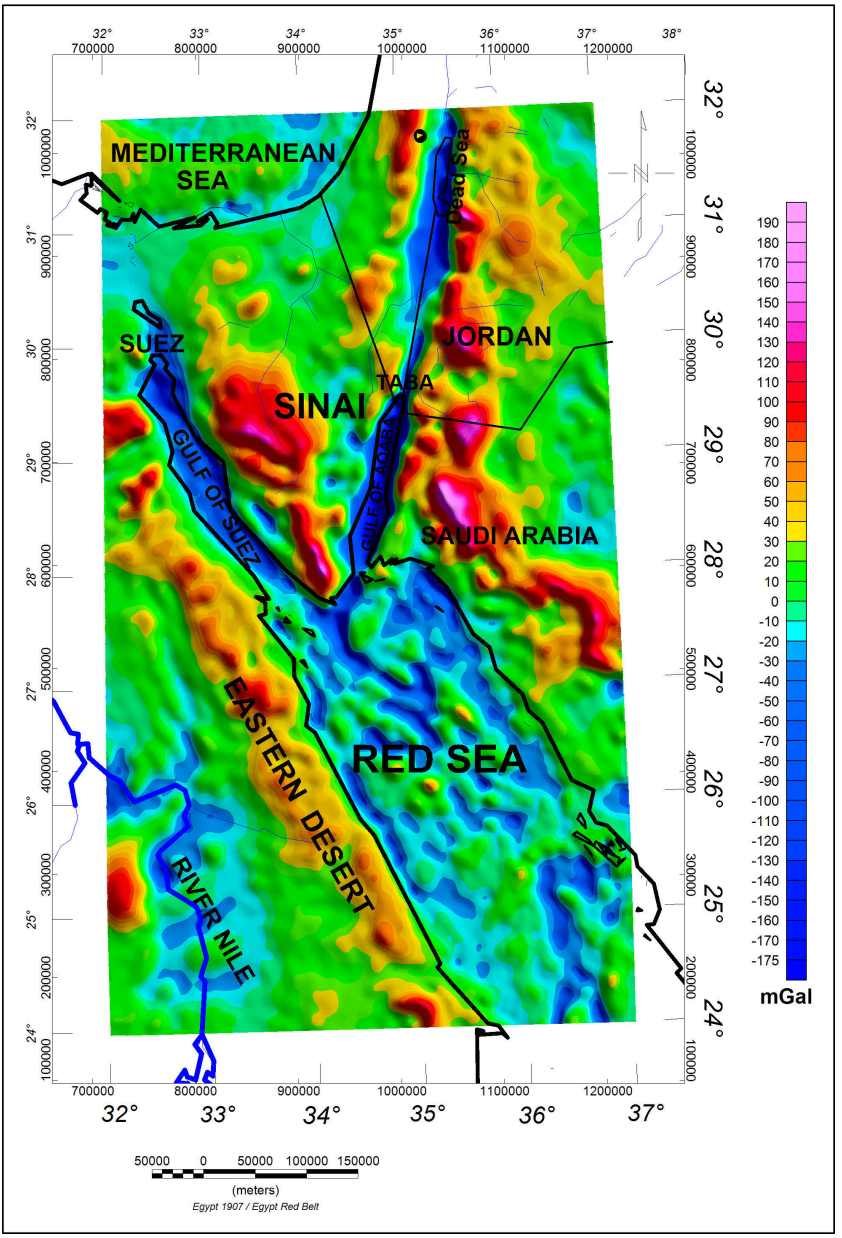

Fig. 9. Satellite Altimetry (Free air) anomaly map of the Northern Red Sea Rift region (derived from *Sandwell and Smith, 1997*).

seismic explosions, deep seismic sounding, shallow refractions, and gravity (e.g., *Drake and Girdler, 1964; Tramontini and Davies, 1969; Makris et al., 1988, 1991; Gaulier et al., 1988; Dorre et al., 1997; Al-Damegh et al., 2005*).

Dorre et al. (1997), Saleh et al. (2006) and Saleh et al. (2013) constructed a crustal thickness map of Egypt, the Red Sea and south-eastern Mediterranean regions using gravity modelling studies. Their results using gravity modelling allowed the construction of a map showing the depth variation of the interface between the upper mantle and the lower crust (Moho depth map). Their estimated Moho depth map is revealed in Figs. 10a and 10b. Nevertheless, *Al-Damegh et al. (2005)* estimated the average crustal thickness of the late Proterozoic Arabian Shield, using seismological data analysis as 39 km. The crust was observed as relatively thin as approximately 23 km along the Red Sea coast. Their study area was extended to the northern part of Red Sea rift region, occupying our study area, as shown in Fig. 10c. Their estimated crustal depths along the Red Sea and Gulf of Aqaba coastal regions are consistent and well correlated with the previous Moho depth that was inferred from the gravity data analysis (e.g. *Dorre et al., 1997* and *Saleh et al., 2006*); see the correlations in Figs. 10a, b, c.

Near the Red Sea, the crust is continental, consisting of a sedimentary layer of 3 km with velocity of 3.5 km/s, overlying a 30 km thickness of crust with moderate velocity changes from 6.0 to 6.35 km/s (*Meshref, 1990*). Near the Nile Valley, the crustal structure is rather heterogeneous and changes abruptly from one area to another. Within the Nile Valley graben, loose water-saturated sediments are present having a rapid decrease in sediment thickness and water saturation in both directions away from the graben (*El-Sayed and Wahlstrom, 1996*). For instance, the type of the crust beneath the eastern Mediterranean Sea varies from oceanic to continental types (*Saleh, 2013*).

The north-western regions of Saudi Arabia are distinct from the Arabian Shield, as this region is characterized by high seismicity in the Gulf of Aqaba and Dead Sea Rift. Active tectonics in this region are associated with the opening of the northern Red Sea and Gulf of Aqaba as well as a major continental strike-slip plate boundary. For comparison purposes, we have also presented a crustal thickness map for the study area (Figs. 10a, 10b and 10c), which clearly reveals northward and eastward trends of the

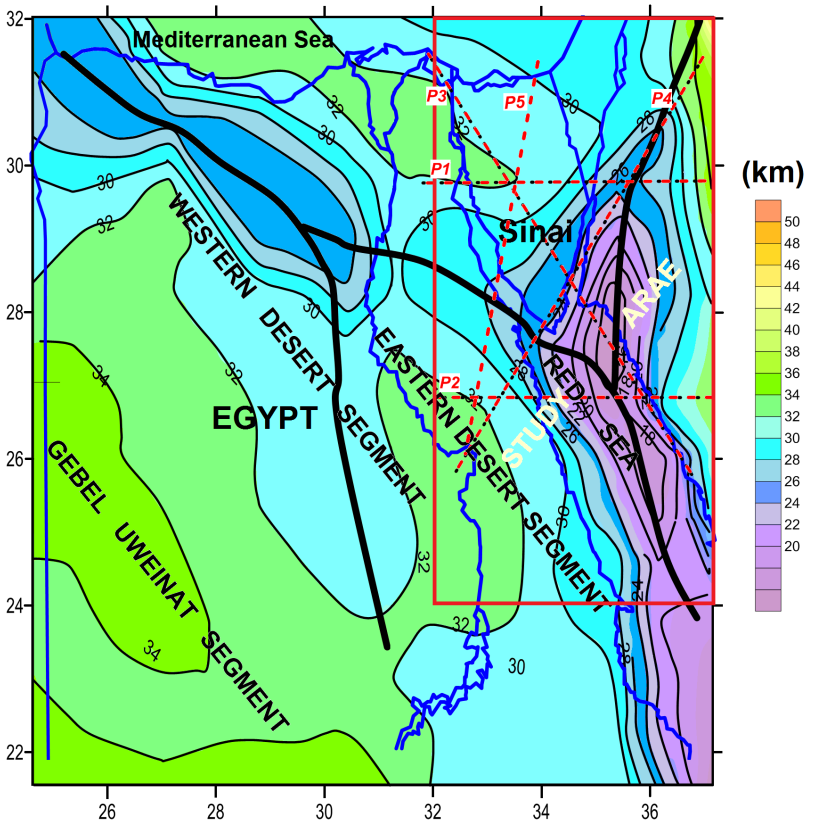

Fig. 10a: Crustal thickness map of Egypt and the adjoining areas as compiled after *Dorre et al. (1997), Saleh (2006), Saleh (2013).* Contour interval: 2 km. The thick curves show the areas of thinned crust. Locations of the sections of Figs. 14a–e are also shown with dashed red lines.

crustal thinning toward the Mediterranean Sea and Red Sea, respectively. This was also observed by *Makris et al. (1988), Marzouk (1988), Dorre et al. (1997), and Seber et al. (2000)* who describe the Egyptian territory as a continental crust with a thickness of 30–34 km, bounded by thin new oceanic crust (< 20 km) that is formed by the Red Sea rifting.

In the Sinai Peninsula, the crust is more or less flat, 32–33 km in thickness, and tends to get thin towards the Gulfs of Suez and Aqaba and towards its southern border where a sudden crustal thinning occurs beneath the northern Red Sea. An additional crustal thickening north-westward is

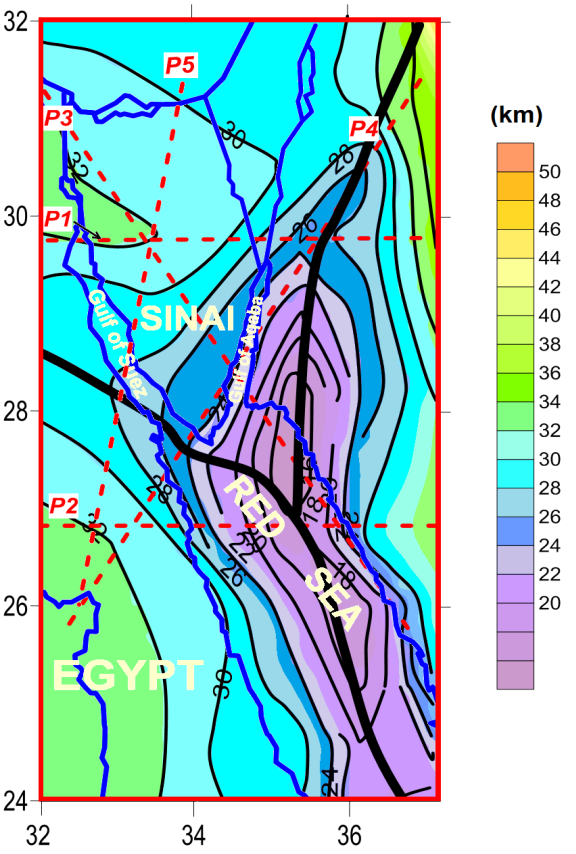

Fig. 10b. Crustal thickness map of Northern Red Sea Rift region derived from Fig. 10a, compiled after *Dorre et al. (1997), Saleh (2006), Saleh (2013)*. Contour interval: 2 km. The thick curves show the areas of thinned crust. Locations of the sections of Figs. 14a–e, are also shown with dashed red lines.

observed in the north-western part of Sinai at the border of the study area.

Generally, we find thicker crust below the Red Sea Mountains compared to the southeastern Mediterranean Basin and Sinai Plateau, but we also find a significantly thin oceanic crustal layer below the northern Red Sea Rift Basin.

The Gulf of Suez and Gulf of Aqaba zones are also underlain by comparable crustal thickness according to their seismic velocities. These findings along with observations in which variations in crustal thickness within each

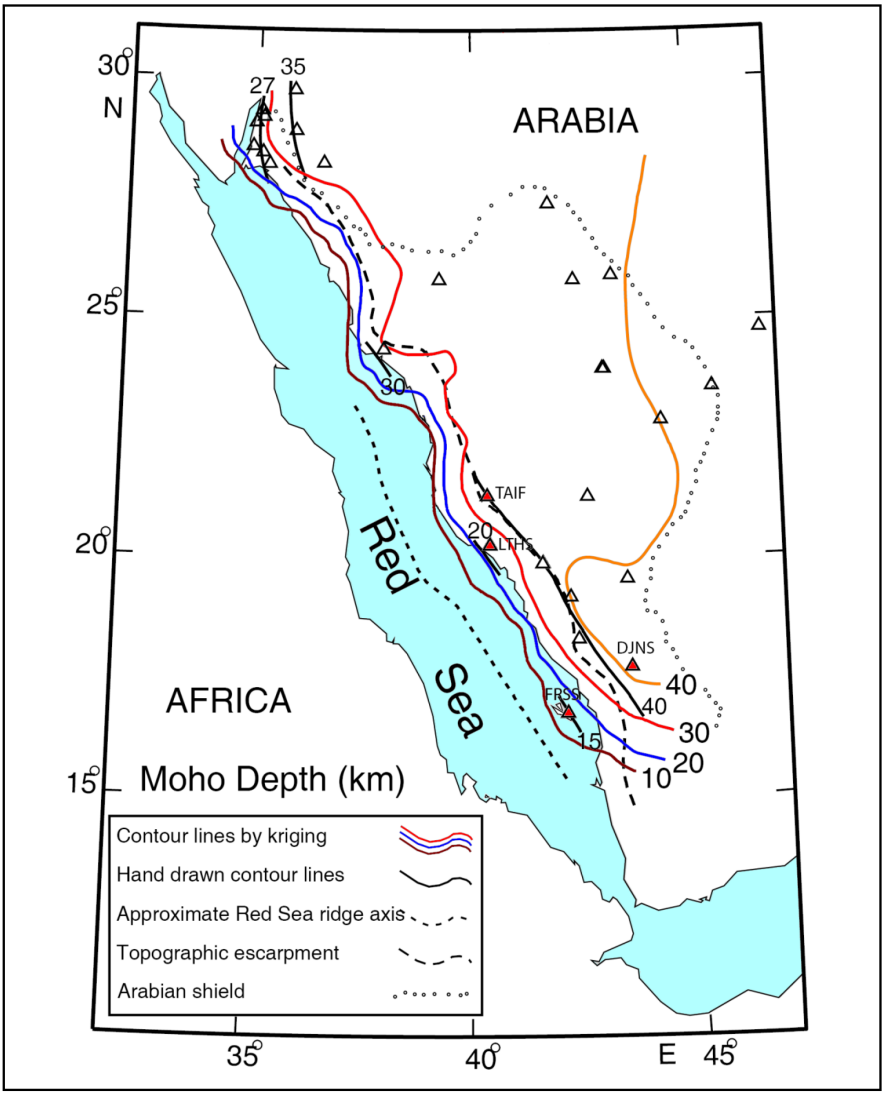

Fig. 10c. Map showing the crustal thickness contour map (Moho depth) of the Arabian Shield region (after *Al-Damegh et al., 2005*). The seismic stations are shown as open triangles. The contour lines based on Kriging approach are shown in different colours, and the hand-drawn contour lines are shown in solid black. The figure also shows the outline of the Arabian Shield (open small circles), the escarpment (long dashes), and the Red Sea ridge (small dashes).

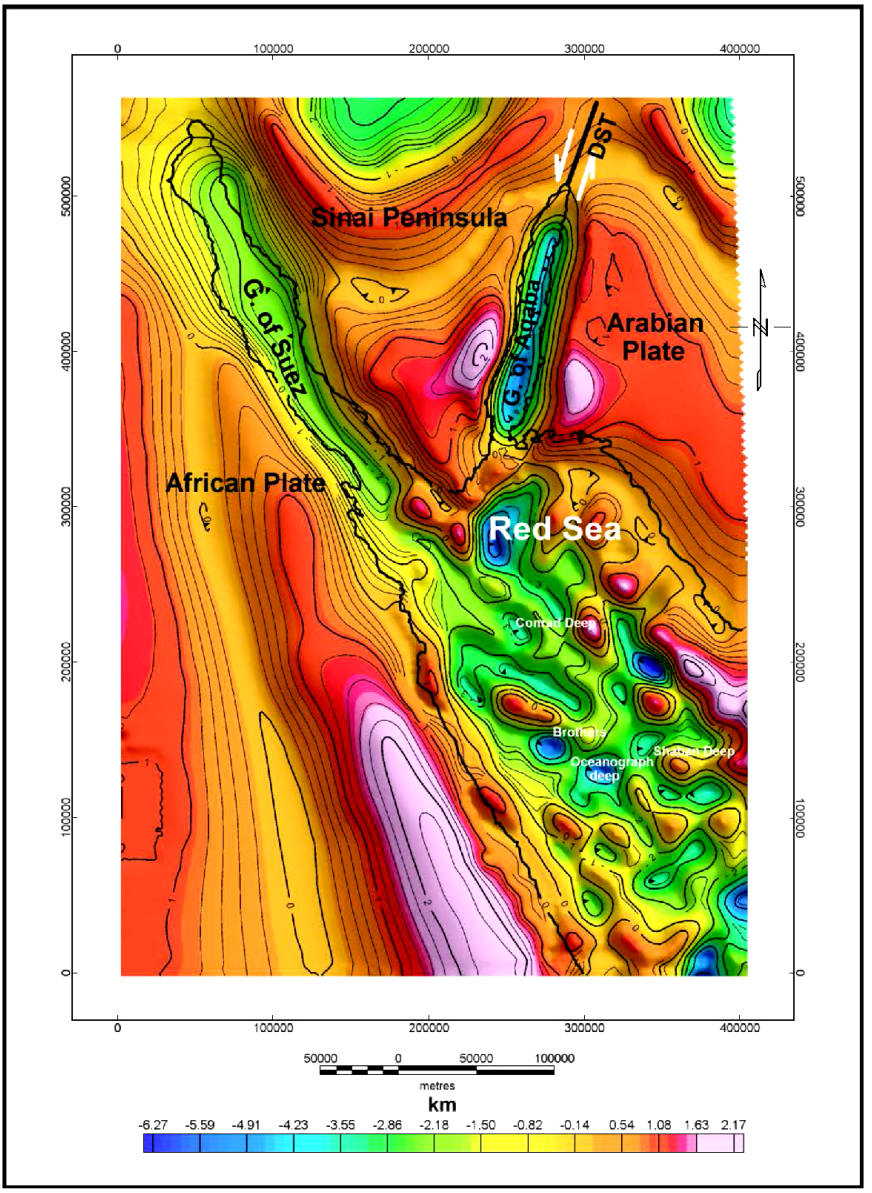

Fig. 11a. Top of the basement map (sedimentary thickness) estimated using well log data, seismic profiles, magnetic and gravity data analysis and 3D geophysical modelling for the northern Red Sea region (after *Saleh, 2009*).

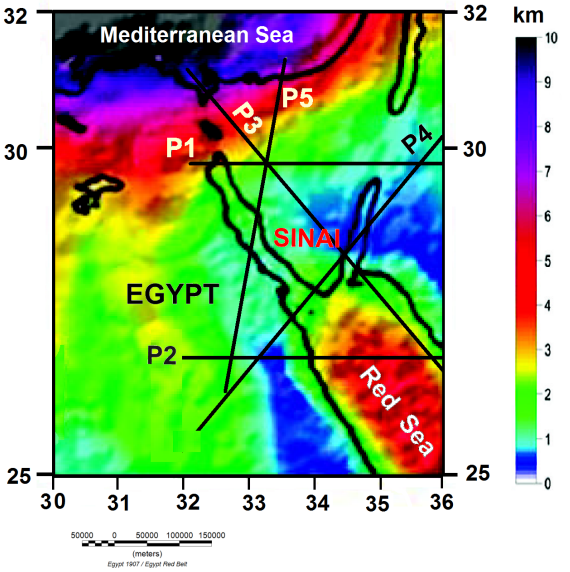

Fig. 11b. Sedimentary thickness map of the Northern Red Sea Rift region compiled after *Laske and Masters (1997)*. Thick curves show the areas of thinned sedimentary cover. Locations of the sections of Figs. 14a–e are also shown with black lines.

tectonic province are well correlated with topography, heat flow, aeromagnetic data and seismological activity indicated that geophysical tools play an important role for distinguishing the various tectonic zones. Thus, our study indicates a broad-scale of correlation between the Bouguer gravity results with other accessible geophysical tools, consequently the estimated tectonic zones in the north-eastern part of Egypt and the Red Sea region.

In addition, *Saleh (2009)* constructed the sedimentary thickness (depth to the basement) for the Northern Red Sea region as shown in Fig. 11a, by applying and reviewing the available relevant information on the Red Sea rift (well logs data, seismic profiles, magnetic and gravity data). Interpretations derived from power spectrum and 3D geophysical modelling methods confirm the depths to the basement-sedimentary contacts derived from the analytical signal and 3D Euler deconvolution techniques. This new compilation enabled significant upgrading of the database for the Northern Red Sea rift region. The basement map of *Saleh (2009)*, was well correlated with that of *Laske and Masters (1997)* as shown in Figs. 11a,b. Both concluded that sedimentary cover is highly correlated for comparison using different

profiles.

Previous studies of heat flow and geothermal regime in Egypt (*Issar et al., 1971; Morgan and Swanberg, 1979; Morgan et al., 1980, 1985; Swanberg et al., 1983; Boulus, 1990; Zaghloul et al., 1995; Hosney, 2000*) related the geothermal features to the tectonic evolution of the area.

The plate margin to the north of Egypt (Fig. 1) appears to be too distant to result in any geothermal anomalies in northern Egypt. The Mediterranean Sea is characterized by heat flow 30–45 $\mathrm{mW\,m^{-2}}$. The low heat flow of the Eastern Mediterranean Sea extends at least as far south as 29° N (*Morgan et al., 1977; Čermák and Hurtig, 1977; Riad et al., 1989*). *Boulos (1990), Morgan et al. (1980, 1983, 1985), Feinstein et al. (1996), Hosney and Morgan (2000), Hosney (2000)* and *Saleh et al. (2013)* studied the heat flow values along the Gulf of Suez and Red Sea.

The Red Sea has developed at a young (25 Ma) spreading axis between the African and Eurasian plate (e.g. *Gaulier et al., 1988; Martinez and Cochran, 1988; Meshref, 1990*). *Girdler and Evans (1977)* showed high heat flow values at the spreading centre of the Red Sea (90% above world mean), and the coast (values are twice of the world mean). *Abdel Zaher et al. (2011)* discovered high heat flow rates in the Gulf of Suez region ($> 100\ \mathrm{mW\,m^{-2}}$). The reasons for high heat flow values in the Red Sea are a thin crust, uplifted basement rocks and a shallow hot mantle. These sources were discovered and interpreted by several authors (*Makris and Ginzburg, 1987; Saleh et al., 2006; Abdel Zaher et al., 2011; Salem et al., 2014*) with gravity, magnetics and seismics.

Morgan et al. (1985) indicated a pattern of low to normal heat flow (35–55 $\mathrm{mW\,m^{-2}}$) inland with high heat flow (75–100 $\mathrm{mW\,m^{-2}}$) in a zone within 30 to 40 km of the coast of the Red Sea. They pointed out a moderately high heat flow (around 70 $\mathrm{mW\,m^{-2}}$) for the Gulf of Suez. Their heat production data indicated that the coastal thermal anomaly is not primarily related to crustal radiogenic heat production. The effects of rapid erosion may contribute to the anomaly, but are not thought to be the primary cause of the anomaly. Alternatively, the anomaly is primarily caused by high mantle heat flow causing lithospheric thinning, centred beneath the Red Sea. The Red Sea is probably underlain by predominantly basic crust, formed either by intrusion into attenuated continental crust or sea-floor spreading, and for most purposes the crust formed in these two modes of

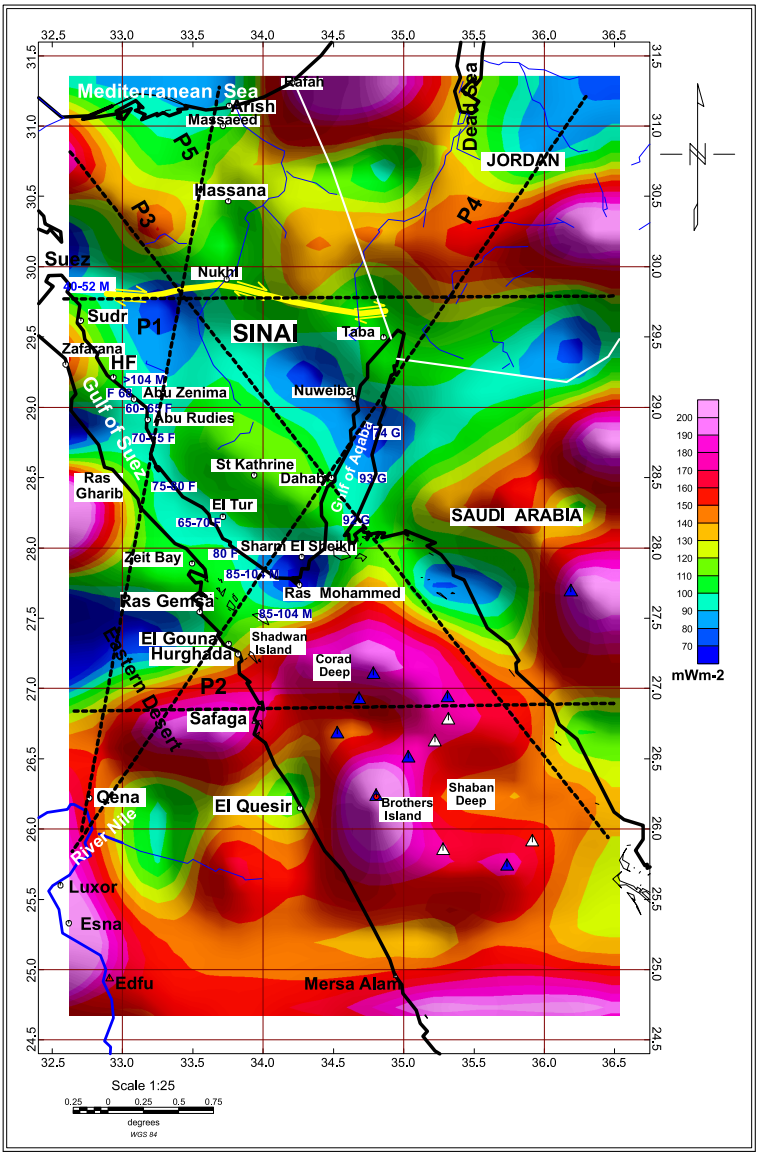

Fig. 12. Heat flow anomaly map the Northern Red Sea Rift region derived from aeromagnetic data analysis (from *Saleh et al., 2013*). Thick curves show the areas of thinned sedimentary cover. Locations of the sections of Figs. 14a–e are also shown with dashed black lines.

extension may be essentially indistinguishable. Contoured heat flow data, from the International Heat Flow Commission, Global Heat Flow Database (http://www.heatflow.und.edu/index2.html), is shown in Fig. 12.

The highest value of heat flow in the eastern part of Egypt was in the Precambrian basement (92 $\mathrm{mW\,m^{-2}}$). Heat flow density in the Red Sea is generally high, reflecting the shallow depth to the asthenosphere and its recent age of intrusions. The early surveys, such as *Girdler and Evans (1977), Haenel (1972), Girdler and Evans (1977)*, reported high heat flow density (HFD) values of approximately 600 $\mathrm{mW\,m^{-2}}$ for the axial trough, whereas the flanks have values of twice the world mean (59 $\mathrm{mW\,m^{-2}}$). The heat flow in the Gulf of Suez could be as high as 80 or even 100 $\mathrm{mW\,m^{-2}}$ (*Morgan et al., 1977; Hosney and Morgan, 2000*). The last value 80–100 $\mathrm{mW\,m^{-2}}$ could be true where it is consistent with the observed low velocity below the Moho in the Gulf of Suez (*Gaulier et al., 1988*) and the mean heat flow of the Red Sea of 116 $\mathrm{mW\,m^{-2}}$ (*Boulus, 1990*). *Saleh et al. (2013)* have evaluated the HFD for the northern Red Sea rift region using magnetic data analysis. They found that the mean values of HFD reached $\sim$160–190 $\mathrm{mW\,m^{-2}}$ along the axial part and active tectonic regions of the Red Sea.

It is a known fact that the part of the mantle at depths below 15 to 17 km is much softened and partially molten which leads to this assumption. Meltings are concentrated at the base of the crust below the deeps. They transport the heat by convection, are responsible for the intrusions in the shallower parts of the crust and the volcanic activity and deliver the thermal energy, which, together with the lateral variation of lithostatic pressure, drives the water circulation in the sediments, where the observed HFD distribution is depressed (*Makris et al., 1991a,b*).

The high level of seismicity along the Gulf of Suez and the Red Sea indicates active tectonics in eastern Egypt (*Kebeasy, 1990*). Geodynamic phenomena are ultimately governed by thermal processes in the Earth's interior. The knowledge of petrophysical properties, like thermal conductivity, P wave velocity and heat generation is very important in the interpretation of terrestrial heat flow patterns and the geothermal processes in the lithosphere. Based on the Cenozoic volcanism along the Red Sea, previous research has argued that the Red Sea is underlain by hot mantle (e.g., *Coleman and McGuire, 1988*). *Ebinger and Sleep (1998)* proposed that rifts may present natural channels for hot material from mantle plumes to flow

horizontally beneath thin lithosphere. The Red Sea has been proposed as such a channel for hot material from the Afar plume to cause the Cenozoic volcanism in western Arabia.

Based on geophysical studies in the territory of Egypt, three major tectonic trends are recognized, namely the Red Sea trend oriented NW–SE, the Gulf of Aqaba trend oriented NE–SW and the Mediterranean trend oriented E–W (*Youssef, 1968*). Owing to these complex tectonics, the distribution of seismic activity in Egypt is observed in four narrow belts: **Levant–Aqaba; Northern Red Sea–Gulf of Suez–Cairo–Alexandria; Eastern Mediterranean–Cairo–Fayum; and the Mediterranean Coastal Dislocation** (*Sieberg et al., 1932; Ismail, 1960; Maamoun et al., 1984; Kebeasy, 1990; Abou Elenean, 1997*). The interaction of the aforementioned tectonics creates continental conditions that are responsible for the major earthquake activity in Egypt.

Significant seismic activity is also found along the entire Gulf of Suez and its extension on the northern part of the Eastern desert towards the Nile Delta along the E–W and WNW faults. This activity trend does not continue further towards the Mediterranean Sea and ceased closer to the west of Nile Valley in the Dahshour area where the 12 October 1992 earthquake (ML5.9) took place.

5. Discussions and conclusions

In this study, we have tried to map and compare the plate boundary between Arabia and Africa at the northern Red Sea rift region including the Suez rift, Gulf of Aqaba-Dead Sea transform and south-eastern Mediterranean region using horizontal gradient gravity data analysis. According to boundary analysis results (as shown in Fig. 6), six distinct provinces (blocks) were identified within the main northern Red Sea rift in the area lies between 24° to 32° N (Fig. 12). The estimated boundary tectonic zones in the present work were classified according to their potential field and heat flow anomaly values, distinctive tectonic trends and thus with regard to the characteristics of their own crustal and sedimentary thicknesses. The evaluated main boundary zones of the present work could be classified as the following zones:

a) The south-eastern Mediterranean tectonic zone (Zone 1)

The south-eastern Mediterranean zone is marked by an east-west trending linear anomaly with high gravity. It is characterized by moderate continental crustal thickness (∼27–29 km) with very thick sedimentary cover (∼ 9 km), as shown in Figs. 10 and 11. This zone is actually traversed by the sub-parallel NE Pelusium megashear system, which extends from Turkey to the South Atlantic. It runs subparallel to the eastern margin of Mediterranean Sea (*Neev et al., 1982*). Indeed, according to the microtectonic analysis (*Eyal and Reches, 1983; Letouzey and Tremolieres, 1980*), they resulted from E–W to WNW–ESE horizontal compression, where this was generally NNW–SSE directed in the Western Desert, shifting progressively to NW in Sinai and nearly E–W in neighbouring regions to the east (*Sehim, 1993*). This eastward increase in the shortening along the Tethyan margins (*Guiraud and Bosworth, 1997*) is synchronous with counterclockwise rotational northward drift of the African-Arabian plate and its increased collisional coupling with the Eurasian plate (*Le Pichon et al., 1988; Ziegler, 1990*). However, distinctive parallel NNW structural trends (Red Sea tectonic trend) were noticed crossing northern Sinai. According to *Ramsay (1986)* and *Camp (1986)* these structural trends were caused by transtensional forces initiated during the Red Sea's evolution and were commonly erupted by Cenozoic basalt flows. *Stern (1985)*, declared that, during the Late Precambrian and Early Cambrian (about 600–540 Ma) extensive left-lateral faulting along the complex NW–SE-trending Najd fault system cut across the Arabian shield. This tectonic episode was accompanied by NW–SE-directed extension in northern Egypt and the Sinai Peninsula.

b) Gulf of Suez tectonic zone (Zone 2)

The Gulf of Suez zone is marked by a (NNW–SSE) trending linear anomaly with gravity low correlates with the proto-Clysmic or Erithrean fractures of *Keely (1994)*. The NNW–SSW trending lineaments chiefly extracted from gravity and the topographic data (Figs. 4 and 8) are notably situated in the Early Cretaceous deposits. This corresponds with the fact that the Red Sea-Gulf of Suez rifting likely commenced in the Cretaceous period (*Makris and Rihm, 1991*) and reached its climax in the Oligocene period, predominantly controlling the linkage of rift-parallel faults in the Gulf of Suez (*Guiraud and Bosworth, 1999*). This zone

is distinguished by moderate continental crustal thickness ($\sim$ 32 km) with thin sedimentary cover ($\sim$ 2–3 km), as shown in Figs. 9 and 10. In fact, subsurface studies conducted onshore just north of the Gulf of Suez (*Moustafa and Khalil, 1995*) argue that the rift was terminated by pre-existing nearly orthogonal structures that were rejuvenated. These structures include the Cairo-Suez fault zone to the west and the Sinai-Negev shear zone to the east (*Moustafa and Khalil, 1995*; Fig. 1).

Saleh et al. (2013) have estimated the heat flow for the northern Red Sea rift region (Fig. 12). They found that the upper northern part of the Gulf of Suez (near Suez city) have a medium heat flow value of 89 mW m^{-2}. However, the Hammam Faroun area (the highest temperature hot spot in Egypt, 70° C), is characterized by a high heat flow value of $\sim$ 104 mW m^{-2}. They have recognized that the heat flow values increase intensively toward the south (toward the marine part of the northern Red Sea along the tip of the Sinai Peninsula).

c) Eastern Desert tectonic zone (Zone 3)

The rocks of the Eastern Desert zone of Egypt form part of the Nubian Shield, a component of the Neoproterozoic Pan-African Orogeny. This zone extends in the south from the northern part of Lake Nasser along the Nile River at 24° N to the Esh El Mallaha boundary line which is located in the north-eastern side close to the Gulf of Suez (Fig. 14). Moreover, it is bordered by the Red Sea on the eastern side. The gravity anomalies of this zone are slightly negative due to its continental crustal thickness which is ranging about 32–38 km thick.

Seismically, this estimated tectonic zone contains many seismic zones according to the classification of *Haggag et al. (2008)*, namely: a) The seismic zone in the Abu-Dabbab area, which is considered the most active zone in the Eastern Desert; many famous earthquakes occurred in this zone. The Abu Dabbab area is considered to be one of the most important active tectonic zones along the Red Sea (*Abu El-Ata, 1987; Badawy et al., 2008; Hussein et al., 2011*). The tectonics of this area were originally controlled by the opening of the Red Sea, which started approximately 30 Ma (e.g., *Martinez and Cochran, 1988*). The extension of the Red Sea led to the origin of several fault zones perpendicular to the Egyptian Red Sea coast from Barnis (near the south-eastern Egyptian border) to the northern Gulf of Suez, which are related to transform

faults. b) The seismic zone containing the activity located in the northern part of the Eastern Desert of Upper Egypt. It can be considered as an active area where many earthquakes were recorded with magnitude ranging up to 4.2. The general trend of the seismicity runs almost N–S.

d) Marine northern Red Sea tectonic zone (Zone 4)

Structurally, the Red Sea is a graben along the crest of an anticline that formed in the Arabian-African Shield. The inner margins of the shield apparently underwent considerable uplift that formed prominent scarps at the edge of the Red Sea rift. A zone of 1–2 km. wide that is composed of high and tensional faults concealed by coastal sediments lies at the foot of the escarpments. On the seaward side of this zone, the basement has been step faulted downward in blocks and lies beneath the shelf area at depths of 2–3 km below sea level (*Chapman, 1978*). Three sets of faults seem to have controlled the development of the Red Sea. These were the NW–SE trending main line of faults which are associated with step faulting and the WNW–ESE major fault trend in the Precambrian basement which caused many irregularities in the coastline (*Chapman, 1978*). Indeed, based on seismicity data, the northernmost part of the Red Sea defines three zones at the entrance of the Gulf of Suez and southern tip of the Sinai Peninsula. The thermal activity and the triple junction nature control the activity in this area. The activity also defines an active trend extending from the southern tip of the Sinai Peninsula to the median zone of the Red Sea. The seismicity of this trend is probably related to the active spreading zone associated with the opening of the Red Sea (*Korrat et al., 2006*). Previous crustal structural results (*Dorre et al., 1997; Saleh et al., 2006*) evaluated the extreme oceanic crustal structures which are flooring the axial trough of the northern Red Sea rift and 30–38 km thick continental crust underneath the Dead Sea rift.

e) Gulf of Aqaba-Dead Sea tectonic zone (Zone 5)

This is considered the most active earthquake zone in Egypt (*Kebeasy, 1990*). This tectonic zone is bounded from the west by the western half of the Sinai Peninsula and by the Arabian Plate from the east. It crosses, through its central part, by a long transform fault zone, extending from Turkey and passing through the Ghab depression in Syria, the Dead Sea, the Gulf of Aqaba, and at last arriving in the floor spreading zone of the Red Sea (*McKenzie, 1970; Dewey et al., 1973*). The latter one

was thought to be the separation between Africa and Arabia (*Cochran, 1981, 1982, 1983*) and it is between the opening of the Gulf of Suez and the predominantly sinistral shear along the Gulf of Aqaba-Dead Sea.
The heat flow values (Fig. 12) in the Gulf of Aqaba appear to increase from north to south. This increase may be related to the more advanced rifting stage of the Red Sea immediately to the south, which presently includes creation of an oceanic crust. This trend also corresponds to the general trend of the deep crustal structure in the gulf (*Ben Avraham and Vonherzen, 1987; Saleh et al., 2013*).

f) North-western region of Saudi Arabia (Tabouk) tectonic zone (Zone 6)

The north-western regions of Saudi Arabia are distinct from the Arabian Shield, as this region is characterized by high seismicity in the Gulf of Aqabah and Dead Sea Rift. Active tectonics in this region are associated with the opening of the northern Red Sea and Gulf of Aqaba as well as a major continental strike-slip plate boundary. The Arabian Plate boundary extends east-north-east from the Afar region through the Gulf of Aden and into the Arabian Sea and Zagros fold belt. The boundary is clearly delineated by teleseismic epicentres, although there are fewer epicentres bounding the eastern third of the Arabian Plate south of Oman. Most seismicity occurs in the crustal part of the Arabian Plate beneath the Zagros folded belt (*Jackson and Fitch, 1981*). *Al-Damegh et al. (2005)* estimated the average crustal thickness of the late Proterozoic Arabian Shield as 39 km. The crust gets thin to approximately 23 km along the Red Sea coast. They observed a shallower Moho for the stations along the Red Sea than in the shield. Moreover, they noticed that the change in the Moho depth becomes more pronounced when they compare stations LTHS and TAIF or FRSS and DJNS in particular (Fig. 10c), where a change of approximately 25 km in Moho depth occurs in a distance of less than 200 km.
Generally the crustal thickness in the Arabian Shield area varies from 35 to 40 km in the west adjacent to the Red Sea to 45 km in central Arabia (*Sandvol et al., 1998; Rodgers et al., 1999*).

In the next step, the Bouguer anomaly field quantities were correlated with the aeromagnetic variation of the heat flow, crustal and sedimentary

thicknesses.

To perform a qualitative interpretation of all available geophysical data sets covering the study area, five profiles were chosen from the Bouguer gravity and magnetic anomaly maps (Figs. 14a–14e); all of them were correlated with the variation in the crustal and sedimentary thicknesses in addition to the heat flow values along the area of the study. The locations of the profiles were chosen in a way that they pass where major estimated boundaries were located.

The study clearly reveals northward and eastward trends of the crustal thinning toward the Mediterranean Sea and Red Sea, respectively. This was also observed by *Makris et al. (1988), Marzouk (1988), Dorre et al. (1997), Seber et al. (2000), Saleh et al. (2006), Abdel-Wahed et al. (2013)* who explained the Egyptian territory as a continental crust with a thickness of 30–34 km, bounded by thin new oceanic crust (< 20 km) that is formed by the Red Sea rifting.

A north-west – south-east trend of crustal thickening covering the northern part of the Western Desert (exhibiting the thickest crust) and coinciding with the Desert Oases, Kharga, Dakhla, and Fayoum depression (Fig. 1). Between the thick crust of the Western desert and the Red Sea, crust tends to thin gently eastward in a north–south lineament trend (Figs. 10a, b). This lineament probably extends northward to the Nile Delta and offshore, where it rapidly loses thickness following the northern coast crustal thinning.

In the Sinai Peninsula, the crust is about 31 km in thickness, and tending to thin toward the Gulfs of Suez and Aqaba and towards its southern border where a sudden crustal thinning occurs down the northern Red Sea. An additional crustal thickening north-westward is observed in the north-western part of Sinai at the border of the study area. In southern Egypt, the crust tends to be thicker near the south-eastern border of the area. It is tempting to speculate that the Red Sea opening may be one of the consequences of the presence of a mega plume that extends from the core-mantle boundary into the upper mantle beneath East Africa, the Red Sea, and the western portion of the Arabian Plate (*Romanowicz and Gung, 2002; Nyblade et al., 2000*).

Generally, the thinned crustal regions are observed where the magnetization value is decreased while the amplitude of the free air anomalies is

increased (*Von Frese et al., 1982; Pamukçu et al., 2007*). Using the same approach, crustal thinning, which is represented as thick curves in Fig. 10, is well interpreted using our investigated profiles as shown in Figs. 13 and 14. In the Sinai Peninsula, the crust is about 31 km thick almost everywhere. It rapidly loses its thickness toward the Gulfs of Suez and Aqaba and toward its southern borders, where a prominent crustal thinning occurs beneath the northern Red Sea (down to 14 km) in north-western Saudi Arabia, southern Palestine and Jordan. It runs parallel to the Aqaba-Levant transform fault system (*Freund, 1965; Girdler and Styles, 1974*). This transform zone has undergone about 100 km of strike-slip and transtensional movement (*Steckler et al., 1988*) and represents the main active seismic zone of the whole area. Positive gravity, negative magnetic anomalies and high heat flow values on the thinned crustal regions (Figs. 14a–14e) suggest that the asthenosphere is uplifted in this region.

Furthermore, an inverse correlation was observed between sediment and crustal thickness, observed in extensional tectonic regimes, where thinned crust acquires a correspondingly thicker sedimentary column especially in continental rift regions. This statement is well correlated for all cross sections in our regional case study (northern Red Sea rift), where thinned crustal regions for selected profiles are always accompanied by thick sedimentary grabens formed under the effect of extensional tectonic regime.

We can conclude that, the plate boundary between Arabia and Africa at the northern Red Sea rift region including the Suez rift, Gulf of Aqaba-Dead Sea transform and south-eastern Mediterranean region was estimated. The boundary analysis method was applied using low pass filtering of gravity data for the northern Red Sea rift region.

Generally, in the delineation and identification of the tectonic zones related to the estimated tectonic boundaries in the northern Red Sea rift, some criteria were followed and utilized as guidelines. These are the geological parameter map of regional tectonics in the area which indicates the location of joints, faults, lineaments, and rift systems that are associated with seismic activities. The boundaries of the tectonic source zones are the results in the inter-agreement of these criteria with the higher priority given to the heat flow and crustal and sedimentary thicknesses with seismic activity. The tectonic zones are selected that are composed of systems of faults or lineaments or rift systems with boundaries that do not generally traverse

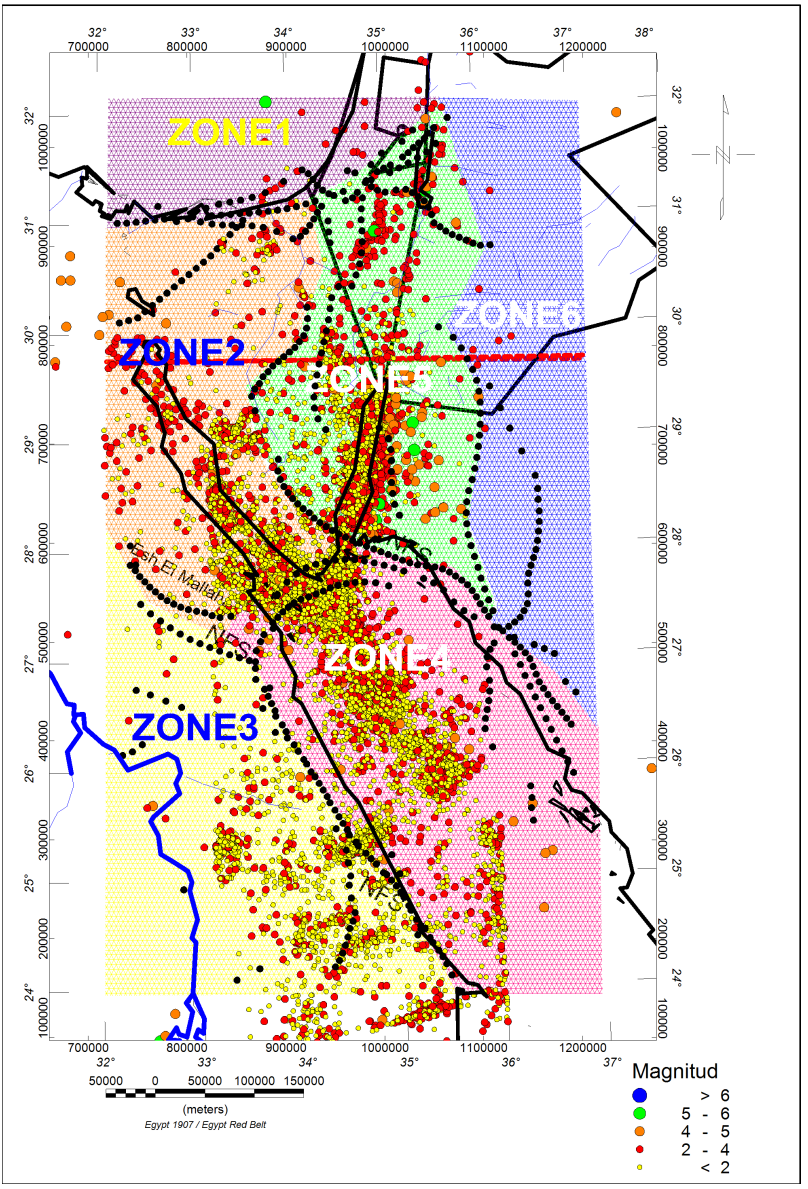

Fig. 13. Tectonic boundary map estimated from Bouguer anomaly map. The area was divided into six tectonic zones (crustal blocks). Seismicity was also located on the map; (seismicity derived from *ENSN, 2008*).

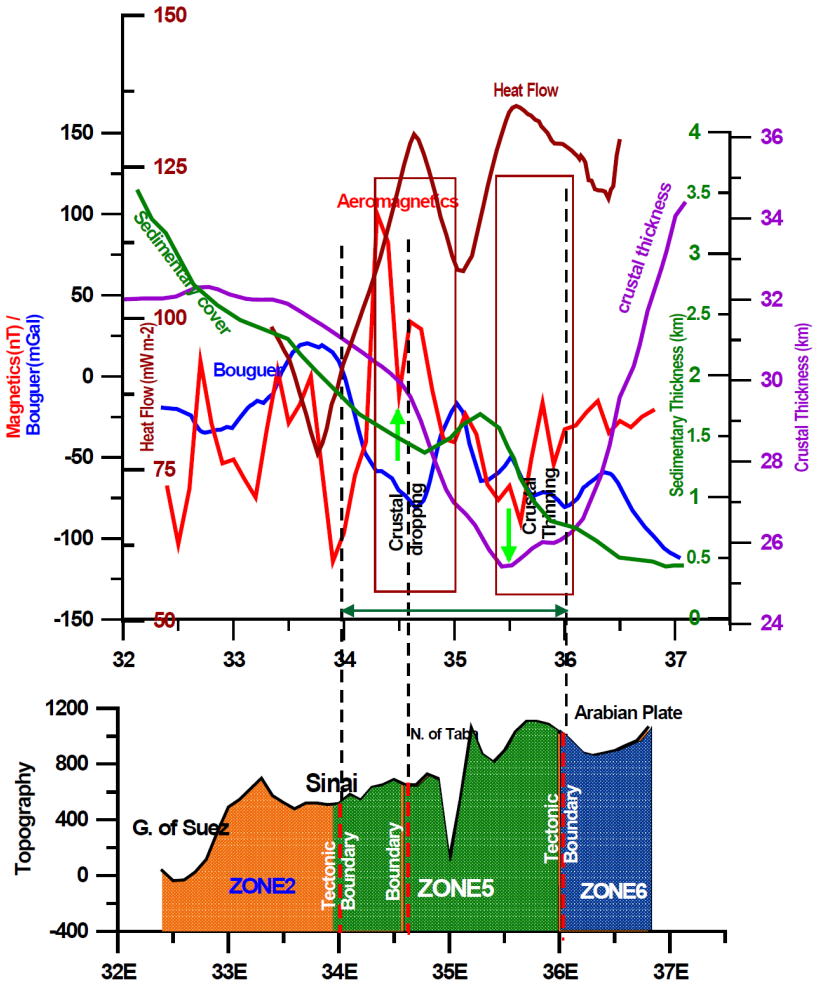

Fig. 14a. Cross-section (P1), Correlation of Bouguer anomaly field quantities with aeromagnetic data, variation of the heat flow, crustal and sedimentary thicknesses. It is 550 km long, starting from the end of Gulf of Suez, crossing central Sinai and ending at the northern part of Gulf of Aqaba in Israel. This Moho depth (crustal thickness) profile is derived from *Dorre et al. (1997)* and shows an abrupt decrease (thinning) in the crustal thickness beneath the northern continental part of the Gulf of Aqaba region (zone 5), with a rapid increase of high heat flow density (HFD) values of approximately 137 mW m^{-2} beneath this crustal thinning region (zone 4).

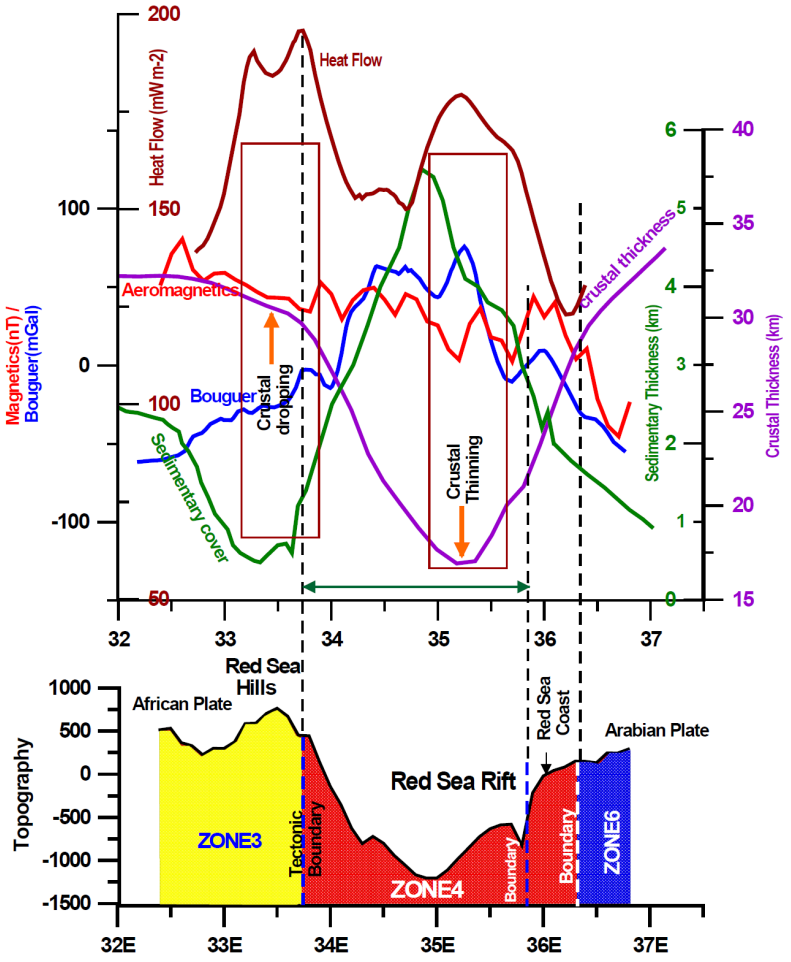

Fig. 14b. Cross-section (P2), Correlation of Bouguer anomaly field quantities with aeromagnetic data, variation of the heat flow, crustal and sedimentary thicknesses. It is 550 km long, starting from the Eastern Desert passing throughout Safaga city, crossing the northern Red Sea rift region and ending in the Arabian plate. The Moho depth (crustal thickness) profile is derived from *Dorre et al. (1997), Saleh et al., (2006)*, shows an abrupt decrease (thinning) in the crustal thickness beneath the northern marine oceanic part of the Red Sea (zone 4), with a rapid increase of heat flow density (HFD) value ($\geq$ 175 mW m^{-2}) beneath this crustal thinning region (zone 4). Moreover, further rapid high heat flow density (HFD) value ($\geq$ 200 mW m^{-2}, of noticeable crustal dropping value) was observed beneath the tectonic boundary region (Red Sea coastal area) between zone 3 and zone 4.

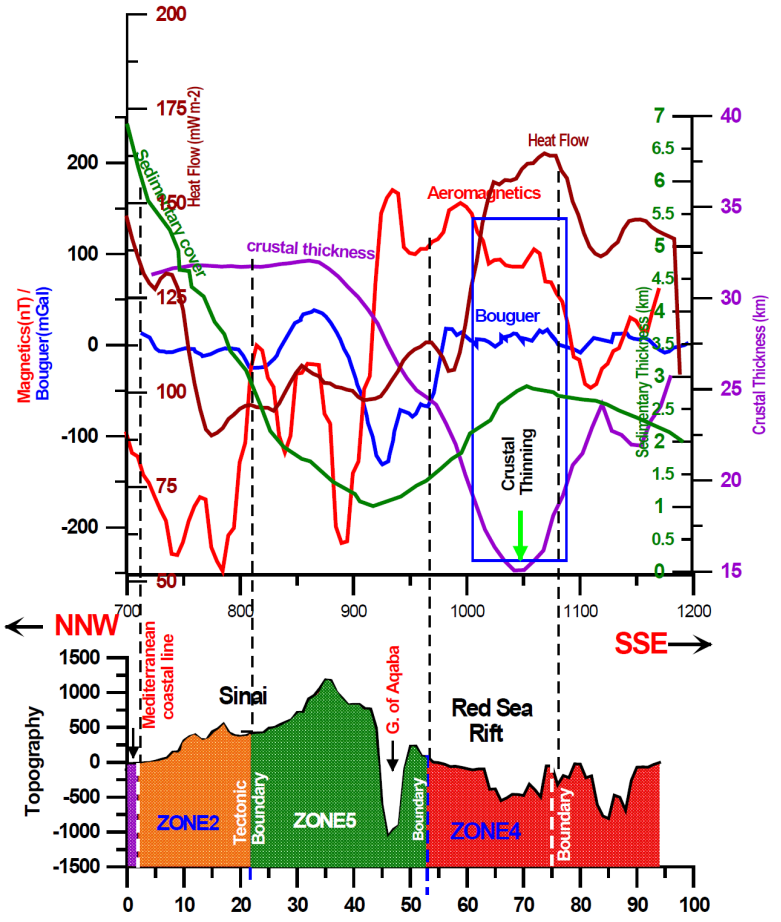

Fig. 14c. Cross-section (P3), Correlation of Bouguer anomaly field quantities with aeromagnetic data, variation of the heat flow, crustal and sedimentary thicknesses. It is 850 km long passing parallel to the Red Sea coast from Arabian side, NW to SE. All the Moho depth (crustal thickness) is derived from *Dorre et al. (1997)*, which shows a decreasing (thinning) in the crustal thickness beneath the Red Sea rift (see P3, Fig. 14c). The Heat flow profile shows a rapid increase to reach maximum value beneath the Red Sea rift region (zone 4). Continuing to the NW direction of the crustal profile (Northern Egypt), the crustal thickness increases rapidly, reaching its maximum value (34 km) beneath northern Sinai (zone 5). In contrast, the heat flow profile shows its minimum value beneath northern Sinai (zone 5). At the end of this profile, the sedimentary cover sequence shows a rapid increase, reaching its maximum value beneath the south-eastern Mediterranean coastal region (zone 2).

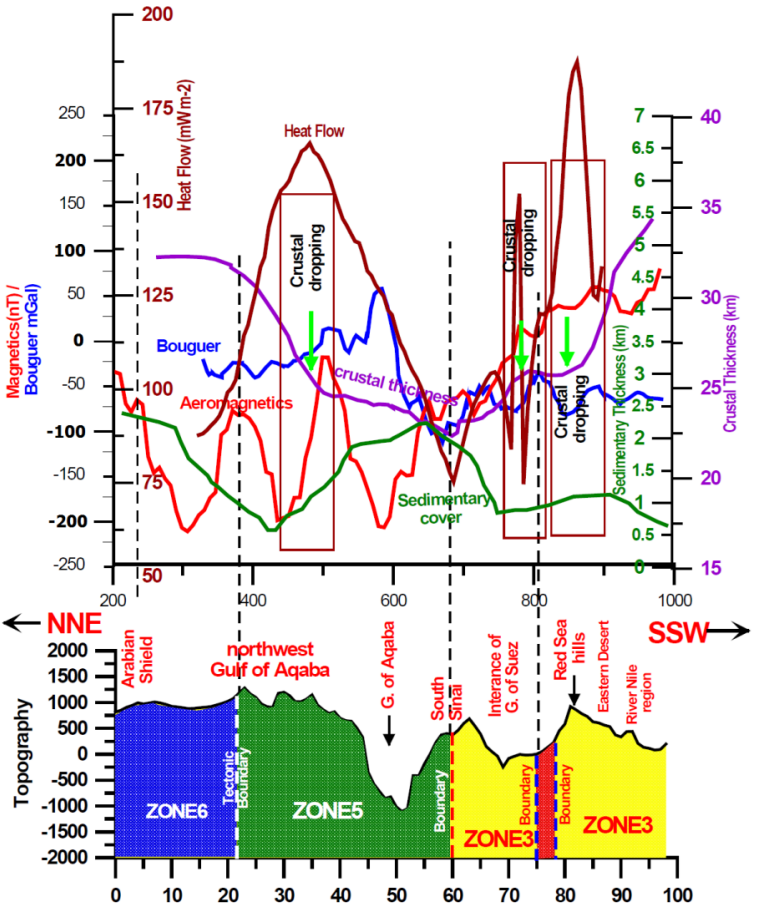

Fig. 14d. Cross-section (P4), Correlation of Bouguer anomaly field quantities with aeromagnetic data, variation of the heat flow, crustal and sedimentary thicknesses. It is about 800 km long crossing the northern Red Sea from SW to NE, passing through Qena city and crossing the northern Red Sea, All the Moho depth (crustal thickness) is derived from *Dorre et al. (1997)*, which shows a decreasing (crustal dropping) in the crustal thickness reached to its minimum value beneath the iterance of the Gulf of Suez and/or Gulf of Aqaba (between zones 3 and 5; see P4, Fig. 13c). However, the heat flow profile shows a rapid increase to reach its maximum value beneath the Red Sea rift region (zone 4). Continuing to the NW direction of crustal profile (Northern Egypt), the crustal thickness increases rapidly, reaching its maximum value (34 km) beneath north Sinai (zone 5). In contracts, the heat flow profile shows its minimum value beneath northern Sinai (zone 5). At the end of this profile, the sedimentary cover sequence shows a rapid increase, reaching its maximum value beneath the south-eastern Mediterranean coastal region (zone 2).

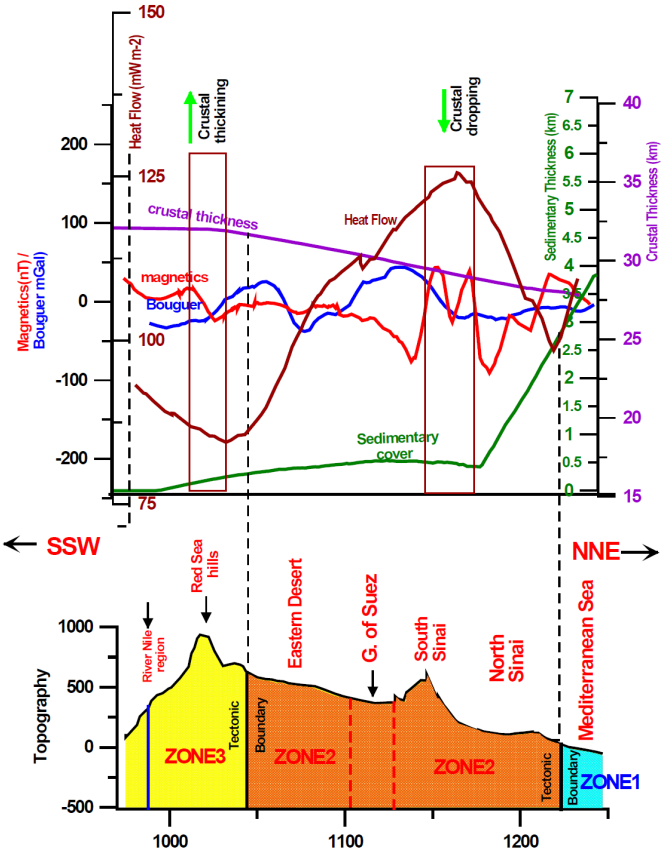

Fig. 14e. Cross-section (P5), Correlation of Bouguer anomaly field quantities with aeromagnetic data, variation of the heat flow, crustal and sedimentary thicknesses. It is nearly 650 km long extending from SSW corner through many famous localities going through Qena city on the River Nile, Red Sea Hills, Eastern Desert and Esh El Melha near the Gulf of Suez, which ends at the Mediterranean coastal region of northern Sinai. The crustal thickness profile shows increasing thickness (crustal thickening) toward the SSW direction with maximum value beneath the Eastern Desert (Red Sea Hills). On the contrary, the sedimentary cover sequence profile shows very thin sedimentary cover and/or cropping out of the basement complex along Eastern Desert and South Sinai. Continuing to the NNW direction of crustal profile (toward the Mediterranean coastal region), the crustal thickness decrease rapidly, reaching its minimum value (28 km) beneath northern Sinai and the Mediterranean coastal region (crustal dropping), with a rapid increase of high heat flow density (HFD) values over 125 mW m^{-2} beneath this crustal thinning region (zone 2). The sedimentary sequences attain their maximum values beneath the South-eastern Mediterranean coastal area (zone 2).

other tectonic units. From these considerations and gravity analysis, six tectonic zones (crustal blocks) were identified and delineated.

Furthermore, it is noted that the regions of intensely thinned crust (especially beneath Sinai and Arabian plate boundary) correspond to areas affected by the Tertiary basaltic volcanism, due to extensional tectonics.

Six heat flow provinces were distinguished: 1) the west of Nile-north of Egypt normal province with low heat flow of about 46 $\mathrm{mW\,m^{-2}}$ and reduced heat flow of 20 $\mathrm{mW\,m^{-2}}$ typical of the Precambrian platform tectonic setting and 2) the eastern Egypt tectonically active province with heat flow up to 80–130 $\mathrm{mW\,m^{-2}}$ including the Gulf of Suez and the northern Red Sea Rift System with reduced heat flow of $>$ 30–40 $\mathrm{mW\,m^{-2}}$, at the transition between the two provinces. The high heat flow of the Gulf of Suez-Red Sea Rift, which is due to anomalous heated upper mantle, falls down laterally to reach the characteristic value of 46 $\mathrm{mW\,m^{-2}}$ at about 90 km away from the Gulf of Suez axes; and about 150–200 km away from the northern Red Sea coast. This marks the limit or the transition zone between the rift tectonic zone and the normal province (zone) of northern Egypt (as shown in profiles 2 and 4 in Figs. 14b and 14d). This result supports the view that the opening of the Red Sea Rift increases south-eastward.

The thinned crustal regions are characterized by decreasing amplitude of magnetic anomalies, which are inversely proportional to the Bouguer gravity anomaly (high gravity values), together with high heat flows and lack of iso-statistic balance. Thus, there is a very clear inverse relationship between surface heat flow and crustal thickness observed in some of the Earth's continental crust regions. Furthermore, this inverse relation between surface heat flow and crustal thickness is also clearly observed along most oceanic crustal structures of the northern Red Sea rift as correlated in Fig. 14e in profile 5.

Acknowledgements. We would like to thank the two anonymous reviewers for their suggestions and for the editorial comments. Also, we would like to express our gratitude to the WGM world Gravity Mapping Project team, conducted by the Bureau Gravimetrique International (BGI), for utilizing the Bouguer gravity data. Finally, we would also like to thank the team of the World Digital Magnetic Anomaly Map project (WDMAM) for providing the magnetic datasets used in the present work. This research was supported by the Slovak Research and Development Agency under the contract No. APVV-16-0482 and Slovak Grant Agency VEGA, grant No. 2/0042/15.

References

Abdel Zaher M., Nishijima J., Fujimitsu Y., Ehara S., 2011: Assessment of low-temperature geothermal resource of Hammam Faraun hot spring, Sinai Peninsula, Egypt. Proceedings, Thirty-Sixth Workshop on Geothermal Reservoir Engineering Stanford University, Stanford, California, January 31 – February 2, 2011.

Abdelwahed M. F., Sami El-Khrepy S., Qaddah A., 2013: Three-dimensional structure of Conrad and Moho discontinuities in Egypt. Journal of African Earth Sciences, **85**, 87–102.

Abou Elenean K., 1997: Seismotectonics of Egypt in Relation to the Mediterranean and Red Seas Tectonics. Ph.D. Thesis, Ain Shams Univ., Egypt.

Abou Elenean K., 2007: Focal mechanisms of small and moderate size earthquakes recorded by the Egyptian National Seismic Network (ENSN), Egypt. NRIAG Journal of Geophysics, **6**, 1, 117–151.

Abu El-Ata A. S. A., 1987: The potential of the seismic interpretation in delineating the shearing deformations and their tectonic implications along the western coast of the Gulf of Suez, Egypt, E.G.S. Proc. of 5th Annual. Meeting, Cairo, Egypt, March 1987, 369–385.

Al-Damegh K., Sandvol E., Barazangi M., 2005: Crustal structure of the Arabian Plate: New constraints from the analysis of teleseismic receiver functions. Earth and Planetary Science Letters, **231**, 177–196.

Allan T. D., Morelli C., 1970: The Red Sea. In: The Sea, 4, part 2, (A. E. Maxwell, ed.) Wiley-Interscience, NY, 493–542.

Badawy A., 2005: Seismicity of Egypt. Seismology Research Letters, **76**, 149–160.

Badawy A., El-Hady S., Abdel-Fattah A. K., 2008: Microearthquakes and neotectonics of Abu-Dabbab, eastern desert of Egypt, Seismol. Res. Lett. **79**(1), 55–67.

Ben-Avraham Z., Vonherzen, R. P., 1987: Heat flow and continental breakup: The Gulf of Elat (Aqaba). J. Geophys. Res.: Solid Earth (1978–2012) 92.B2 (1987): 1407–1416.

Ben-Avraham Z., 1985: Structural Framework of the Gulf of Elat (Aqaba), Northern Red Sea. J. Geophys. Res,., **90**, 703–726.

Ben-Menahem A., Nur A., Vered M., 1976: Tectonics, seismicity and structure of the Afro-Eurasian junction-the breaking of an incoherent plate. Physics and Earth Planet Interiors, **12**, 1–50.

Blakely R. J., Simpson R. W., 1986: Approximating edges of source bodies from magnetic or gravity anomalies. Geophysics, **51**(7), 1494–1498.

Boulos F. K., 1990: Some aspects of the geophysical regime of Egypt in relation to heat flow, groundwater and microearthquakes, in R. Said (ed.), The Geology of Egypt, A. A. Balkema, Rotterdam, 61–89.

Camp V. E., 1986: Geologic map of the Umm Birak quadrangle, sheet 23D, Kingdom of Saudi Arabia (with text). Saudi Arabian Deputy Ministry for Mineral resources Geoscience Map GM 87, scale 1:250000, 40 p.

Čermák V., Hurtig E., 1977: Preliminary heat flow map of Europe 1:5000000. IASPEI – Heat Flow Commission, Potsdam, GDR.

Cochran J. R., Karner G. D., 2007: Constraints on the deformation and rupturing of continental lithosphere of the Red Sea: the transition from rifting to drifting. In: Karner G. D., Manatschal G., Pineheiro L. M. (eds) Imaging, Mapping and Modelling Continental Lithosphere Extension and Breakup. Geological Society, London, Special Publications, **282**, 265–289. doi: 10.1144/SP282.13.

Cochran J. R., 1983: A model for the development of Red Sea. Bulletin American Petroleum. Geology **67**(1), 41–69.

Cochran J. R., 2005: Northern Red Sea: Nucleation of an oceanic spreading center within a continental rift, G3 (Geochemistry, Geophysics, Geo-systems). J. Earth Sci., **6**(3), 34.

Cochran J. R., Gaulier, J. M., LePichon X., 1991: Crustal structure and the mechanism of extension in the northern Red Sea: Constraints from gravity anomalies. Tectonics, **10**, 1018–1037.

Cochran J. R., Martinez F., Steckler M. S., Hobart M. A., 1986: Conrad Deep: A new Northern Red Sea Deep Origin and implications for continental rifting. Earth Planet. Sci. Lett., **78**, 18–32.

Cochran J. R., 1981:The Gulf of Aden, structure and Evolution of young ocean basin and continental margins. J. Geophys. Res. **86**, 263–288.

Cochran J. R., 1982: The magnetic quiet zone in the eastern Gulf of Aden, implications for the early development of the continental margins. Geophysical. Journal Royal Astronomical Society, **68**, 171–201.

Coleman R. G., McGuire A. V., 1988: Magma systems related to the Red Sea opening. Tectonophysics, **150**, 12, 77–100.

Cordell L., Grauch V. J. S., 1982: Reconciliation of the discrete and integral Fourier transforms. Geophysics, **47**, 237–243.

Cordell L., Grauch V. J. S., 1985: Mapping basement magnetization zones from aeromagnetic data in the Saint Juan Basin, New Mexico. In: (William J. Hinze, Ed.), The Utility of Regional Gravity and Magnetic Anomaly Maps. SEG, Tulsa, OK, pp. 181–197.

Dewey J. F., Pitman W. C., Ryan, W. B. F., Bonnin J., 1973: Plate tectonics and the evolution of the Arabian Plate system. Bulletin Geological Society America, **84**, 3137–3180.

Dorre A. S., Carrara E., Cella F., Grimaldi M., Hady Y. A., Hassan H., Rapolla A., Roberti N., 1997: Crustal thickness of Egypt determined by gravity data. Journal of African Earth Sciences **25**(3), 425–434.

Drake C. L., Girdler R. W., 1964: A Geophysical Study of the Red Sea. Geophysical Journal International, **8**, 5, 473–495.

Ebinger C. J., Sleep N. H., 1998: Cenozoic magmatism throughout east Africa resulting from impact of a single plume. Nature, **395**, 788-791.

EGPC, (Eyptian General Petroleum Cooperation), 1990: Aeromagnetic Map for Sinai Peninsula (scale 1:100 000).

EGSMA (Egyptian Geological Survey and Mining Authority), 1993: Geological and geophysical studies for groundwater exploration on Nukhl area, central Sinai. Internal report No. 49/93, 24p.

Ekinci Y. L., Yiditba E., 2012: A geophysical approach to the igneous rocks in the Biga Peninsula (NW Turkey) based on airborne magnetic anomalies: geological implications. Geodinamica Acta, **25**(3–4), 267–285.

Ekinci Y. L., Yiditba E., 2015: Interpretation of gravity anomalies to delineate some structural features of Biga and Gelibolu peninsulas, and their surroundings (northwest Turkey). Geodinamica Acta, **27**(4), 300–319.

El-Sayed A., Wahlstrom R., 1996: Distribution of the energy release, b-values and seismic hazard in Egypt. Natural Hazards, **13**, 2, 133–150.

El Shazly E. M., 1977: In: The Ocean Basin and Margins. The Eastern Mediterranean, A.E.M Nairn, WH Kanes, F.G. Stehli eds, **4**a.

El-Geziry M. V., Marzouk I. M., 1974: Miocene rock stratigraphy of Egypt. Egypt Journal of Geology, **18**, 1–59.

ENSN, 2008: Egyptian National Seismological Network Report.

Eyal Y., Reches Z., 1983: Tectonic analysis of the Dead Sea Rift region since the Late Cretaceous based on mesostructures. Tectonics, **2**, 167–185.

Feinstein S., Kohn B. P., Steckler M. S., Eyal M., 1996: Thermal history of the eastern margin of the Gulf of Suez, I. Reconstruction from borehole temperature and organic maturity measurements. Tectonophysics, **266**, 203–220.

Folkman Y., Assael R., 1980: *Sinai Gravity Map*, Institute for Petroleum Researchand Geophysics, Israel, Scale 1:500,000.

Freund R., 1965: A model for the structural development of Israel and adjacent areas since upper Cretaceous times. Geological Magazine, **102**, 190–205.

Gaulier J. M., Le Pichon X., Lyberis N., Avedik F., Geli L., Moretti I., Hafez S., 1988: Seismic study of the crustal thickness, Northern Red Sea and Gulf of Suez. Tectonophysics, **153**, 55–88.

Geosoft Oasis montaj software, version 7.2, 2008: Software for Earth Science Mapping and Processing.

Ginzburg A., Folkman Y., Rybakov M., Rotstein Y., Assael Y., Yuval Z., 1993: Israel: Bouguer Gravity Map, scale 1:250,000. Survey of Israel.

Girdler R. W., Styles P., 1974: Two stages in the Red Sea floor spreading. Nature, **247**, 7–11.

Girdler R. W., Evans T. R., 1977: Red Sea heat flow. Geophysical Journal International, **51**, 245–251.

Guennoc P., Pautot G., Le Quentric M. F., Coutelle A., 1990: Structure of an early oceanic rift in the northern Red Sea. Oceanologica Acta, **13**, 145–155.

Guiraud R., Bosworth W., 1997: Senonian basin inversion and rejuvenation of rifting in Africa and Arabia: synthesis and implications to plate-scale tectonics. Tectonophysics, **282**, 39–82.

Guiraud R., Bosworth W., 1999: Phanerozoic geodynamic evolution of northeastern Africa and the northwestern Arabian platform. Tectonophysics, **315**, 73–108.

Haenel R., 1972: Heat flow measurements in the Red Sea and Gulf of Aden. Z. Geophys., **38**, 1035–1047.

Haggag H. M., Gaber H. H., Sayed A. D., Ezzat M. E., 2008. A review of the recent seismic activity in the southern part of Egypt (Upper Egypt). Acta Geodyn Geomater, **1**, 19–29.

Hammer S., 1939. Terrain corrections for gravimeter stations. Geophysics **4**, 184–194.

Hosney H. M., Morgan P., 2000: Geothermal behavior and tectonic setting in the Northern Gulf of Suez, Egypt. Journal of Environmental Sciences. **19**, 55–74.

Hosney H. M., 2000: Geophysical parameters and crustal temperatures characterizing tectonic and heat flow provinces of Egypt, ICEHM 2000, Cairo University, Egypt, 152–166.

Hussein H. M., Moustafa S. S. R., Elawadi E., Al-Arifi N. S., Hurukawa N., 2011: Seismological aspects of the Abou Dabbab region, Eastern Desert, Egypt. Seismol. Res. Lett. **82**(1), 81–88.

Ismail A., 1960: Near and Local Earthquakes at Helwan from 1903–1950, Helwan Observatory Bulletin, **49**.

Issar A., Rosenthal E., Eckstein Y., Bogoch R., 1971: Formation waters, hot springs and mineralization phenomena along the eastern shore of the Gulf of Suez. International Association of Scientific Hydrology Bulletin, **16**, 25–44.

Jackson J., Fitch T., 1981: Basement faulting and the focal depths of the larger earthquakes in the Zagros mountains (Iran). Geophysical Journal International, **64**, 561–586.

Kamel K., 1990. Gravity map. In: Said R. (Ed.), The Geology of Egypt. A. A. Balkema, Rotterdam, 45–50.

Kebeasy R. M., 1990: Seismicity. The Geology of Egypt, Balkema, Rotterdam, 51–59.

Keely M. L., 1994: Phanerozoic evolution of the basins of Northern Egypt and adjacent areas. Geologische Rundschau, **83**(4), 728–742.

Knott S. T., Bunce E. T., Chase R. L., 1966: Red Sea seismic reflection studies. Geological Survey of Canada, **66**, 33–61.

Korrat I. M., Hussin H. M., Marzouk I., Ibrahim E. M., Abdel-Fattah R., Hurukawa N., 2006: Seismicity of the northernmost part of the Red Sea (1995–1999). Acta Geophysica, **54**, 33–49.

Laske G., Masters G., 1997: A global digital map of sediment thickness. EOS Transactions, **78**, F483.

Le Pichon X., Francheteau J., 1978: A plate tectonic analysis of the Red Sea-Gulf of Aden area. Tectonophysics, **46**, 369–406.

Le Pichon X., Gaulier J. M., 1988: The rotation of Arabia and the Levant fault system. Tectonophysics **153**, 271–294.

Le Pichon X., Bergerat E., Roulet M. J., 1988: Plate kinematics and tectonics leading to the Alpine belt formation; a new analysis. Geological Society of America Special Papers, **218**, 111–131.

Letouzey J., Tremolieres P., 1980: Paleo-Stress Fields around the Mediterranean since the Mesozoic from Microtectonics. Comparison with Plate Tectonic Data. Rock Mechanics Supplement, **9**, 173–192.

Maamoun M., Megahed A., Allam A., 1984: Seismicity of Egypt. Bulletin of Helwan Institute of Astronomy and Geophysics, **4**(B), 109–162.

Makris J., Rihm R., 1991: Shear-controlled evolution of the Red sea: pull apart model. Tectonophysics **198**(2–4), 441–466.

Makris J., Ginzburg A., 1987: The Afar depression: transition between continental rifting and sea-floor spreading. Tectonophysics **141**, 199–214.

Makris J., Henke C. H., Egloff F., Akamaluk T., 1991a: The gravity field of the Red Sea and East Africa. In: J. Makris, P. Mohr and R. Rihm (Ed). Tectonophys, **198**, 369–382.

Makris J., Rihm R., Allam A., 1988: Some geophysical aspects of the evolution and structure of the crust in Egypt. In: Greiling, S. E.-G.a. R. O. (Ed.), The Pan-African Belt of Northeast Africa and Adjacent Areas, Tectonic Evolution and Economic Aspects of a Late Proterozoic Orogen: Braunschweig, Friedr. Vieweg and Sohn, pp. 345–369.

Makris J., Tsironidis J., Richter H., 1991b: Heat flow density distribution in the Red Sea. In: J. Makris, P. Mohr and R. Rihm (Ed), Red Sea: Birth and Early History of a New Oceanic Basin. Tectonophysics, **198**, 383–393.

Makris J., Wang J., 1994: Bouguer gravity anomalies of the eastern Mediterranean Sea. In: Krasheninnikov V. A., Hall, J. K. (Eds.), Geological Structure of the Northeastern Mediterranean (Cruise 5 of the Research Vessel "Akademik Nikolaj Strakhov"). Historical Production Hall Ltd., Jerusalem. pp. 87–98.

Martinez F., Cochran J. R., 1988: Structure and tectonics of the northern Red Sea: Catching a continental margin between rifting and drifting. Tectonophysics, **150**, 1–32.

McClusky S., Balassanian S., Barka A., Demir C., Ergintav S., Georgiev I., Gurkan O., Hamburger M., Hurst K., Kahle H., Kastens K., Kekelidze G., King R., Kotzev V., Lenk O., Mahmoud S., Mishin A., Nadariya M., Ouzounis A., Paradissis D., Peter Y., Prilepin M., Reilinger R., Sanli I., Seeger H., Tealeb A., Toksoz M. N., Veis G., 2000: Global positioning system constraints on plate kinematics and dynamics in the eastern Mediterranean and Caucasus. Journal of Geophysical Research, **105**(3), 5695–5719.

McClusky S. C., Reilinger R. E., Mahmoud S., Ben Sari D., Tealeb, A., 2003: GPS constraints on Africa (Nubia) and Arabia plate motions. Geophysical Journal International, **155**, 126–138.

McKenzie D. P., Davies D., Molnar P., 1970: Plate tectonics of the Red Sea and East Africa. Nature **226**, 243–248.

Meshref W. M., 1990: Tectonic Framework. In: Said, R. (Ed.), The Geology of Egypt. A. A. Balkema Publishers, Rotterdam, Netherlands, 113–156.

Minich G., 1987. Gravimetrische Messungen im nordischen Roten Meer, Diplomarbeit, Institut für Geophysik, Universität Hamburg, 73 Seiten, unpublished.

Morgan P., Swanberg C., 1979: Heat Flow and the Geothermal Potential of Egypt. Pageoph, 117 (1978/1979), 213–225. Birkhauser Verlag, Basel.

Morgan P., Blackwell D. D., Farris J. C., Boulos F. K., Salib P. G., 1977: Preliminary geothermal gradient and heat flow values for northern Egypt and the Gulf of Suez from oil well data, in Proceedings, Int. Cong. Thermal Waters, geothermal Energy and Volcanism of the Mediterranean Area, Nat. Tech. Univ., Athens, Greece, **1**, 424–438.

Morgan P., Boulos F. K., Swanberg C. A., 1983: Regional geothermal exploration in Egypt. Geophysical Prospecting, **31**, 361–376.

Morgan P., Boulos F. K., Hennin S. F., EI-Sherif A. A., El-Sayed A. A., Basta N. Z., Melek Y.S., 1985: Heat flow in Eastern Egypt: The thermal signature of a continental breakup. Journal of Geodynamics, **4**, 107–131.

Morgan P., Swanberg C. A., Boulos F. K., Hennin S. F., El-Sayed A. A., Basta N. Z., 1980: Geothermal studies in northeast Africa. Annals of Geological Survey of Egypt, **10**, 971–987.

Moustafa A. R., Khalil H. M., 1995: Superposed deformation in the northern Suez Rift, Egypt: relevance to hydrocarbons exploration. Journal of Petroleum Geologists, **18**(3), 245–266.

Neev D., 1975: Tectonic Evolution of the Middle East and the Levantine Basin (Eastern Most Mediterranean). Geology, **3**, 12, 683–686.

Neev D., Hall J. K., Saul J. M., 1982: The Pelusium megashear system across Africa and associated lineament swarms. Journal of Geophysical Research, **87**, 1015–1030.

Nyblade A. A., Owens T. J., Gurrola H., Ritsema J., Langston C. A., 2000: Seismic evidence for a deep upper mantle thermal anomaly beneath east Africa. Geology, **28**, 599–602.

Pamukçu O. A., Akçiğ Z., Demirbas S., Zor E., 2007: Investigation of crustal thickness in Eastern Anatolia using gravity, magnetic and topographic data. Pure and Applied Geophysics **164**, 2345–2358.

Piersanti A., Nostro C., Riguzzi F., 2001: Active displacement field in the Suez-Sinai area: The role of postseismic deformation. Earth and Planetary Science Letters, **193**, 13–23.

Ramsay C. R., 1986: Geologic map of the Rabigh quadrangle, sheet 22D. Kingdom of Saudi Arabia (with text). Saudi Arabian deputy Ministry for Mineral Resources Geoscience Map GM-84, scale 1:250,000, 49 p.

Riad S., Abdelrahman E., Refai E., Ghalban H., 1989: Geothermal studies in the Nile Delta, Egypt. Journal of African Earth Sciences (and the Middle East), **9**, 637–649.

Riad S., 1977: Shear Zones in North Egypt Interpreted from Gravity Data. Geophysics, **42**, 1207–1214.

Rodgers A., Walter W., Mellors R., Al-Amri A. M. S., Zhang Y. S., 1999: Lithospheric structure of the Arabian Shield and Platform from complete regional waveform modeling and surface wave group velocities. Geophysical Journal International, **138**, 871–878.

Roeser H. A., 1975: A detailed magnetic survey of the southern Red Sea. Geol Jahrb **13**, 131–153.

Romanowicz B., Gung Y., 2002: Superplumes from the core-mantle boundary to the lithosphere: Implications for heat flux. Science, **296**, 513–516.

Rybakov M., Goldshmidt V., Rotstein Y., 1997: New compilation of the gravity and magnetic maps of the Levant. Geophys. Res. Lett. **24**, 33–36.

Said R., 1962: The Geology of Egypt. 376 p. Elsevier, Oxford.

Said R., 1963: Structure setting of the Gulf of Suez, 6th World Petroleum Congress Proceedings, Frankfurt.

Saleh S., 2009: Basement Configureuration of the Northern Red Sea and Gulf of Suez regions, from geophysical data. Journal of Applied Geophysics (ESAP-Egypt), **8**(1), 311–329.

Saleh S., 2013: 3D crustal and lithospheric structures in the southeastern Mediterranean and northeastern Egypt. Pure Appl. Geophys., **170**, 2037–2074. Springer Basel, doi: 10.1007/s00024-013-0673-y.

Saleh S., Jahr T., Jentzsch G., Saleh A., Abou Ashour N. M., 2006: Crustal evaluation of the Northern Red Sea rift and Gulf of Suez, Egypt from geophysical data: 3-dimensional modeling. Journal of African Earth Sciences **45**, 257–278.

Saleh S., Salk M., Pamukçu O., 2013: Estimating Curie point depth and heat flow map for northern Red Sea rift of Egypt and its surroundings, from aeromagnetic data. Pure and Applied Geophysics, **170**(5), 863–885, doi: 10.1007/s00024-012-0461-0.

Salem A., Green C., Ravat D., Singh K. H., East P., Fairhead D., Mogren S., Biegert E., 2014: Depth to Curie temperature across the central Red Sea from magnetic data using the defractal method. Tectonophysics, doi: 10.1016/j.tecto.2014.04.027.

Sandvol F., Seber D., Barazangi M., Vernon F., Mellors R., Al-Amri A., 1998: Lithospheric velocity discontinuities beneath the Arabian Shield. Geophysical Research Letters, **25**, 2873–2876.

Sandwell D. T., Smith W. H. F., 1997: Marine gravity anomaly from Geosat and ERS 1 Satellite altimetry. Journal of Geophysical Research, **102**, 10039–10054.

Seber D., Steer D., Sandvol E., Sandvol C., Brindisi C., Barazangi M., 2000: Design and development of information systems for the geosciences: An application to the Middle East. GeoArabia, **5**(2), 269–296.

Segev A., Rybakov M., Lyakhovsky V., Hofstetter A., Tibor G., Goldshmidt V., Ben Avraham Z., 2006. The structure, isostasy and gravity field of the Levant continental margin and the southeast Mediterranean area. Tectonophysics, **425**, 137–157, doi: 10.1016/j.tecto.2006.07.010.

Sehim A., 1993: Cretaceous tectonics in Egypt. Egyptian Journal of Geology, **37**, 335–372.

Sieberg A., 1932: Untersuchungen über Erdbeben und Bruchschollenbau im östlichen Mittelmeergebiet: Ergebnisse einer erdbebenkundlichen Orientreise, unternommen im Frühjahr 1928 mit Mitteln der Notgemeinschaft der deutschen Wissenschaft. G. Fischer (in German).

Steckler M. S., Berthelot F., Lyberis N., LePichon X., 1988. Subsidence in the Gulf of Suez: implications for rifting and plate kinematics, Tectonophysics, **153**, 249–270.

Steckler M. S., Feinstein S., Kohn B. P., Lavier L. L., Eyal M., 1998: Pattern of mantle thinning from subsidence and heat flow measurements in the Gulf of Suez: Evidence for the rotation of Sinai and along-strike flow from the Red Sea. Tectonics, **17**, 903–920.

Stern R. J., 1985: The Najd Fault System, Saudi-Arabia and Egypt – A Late Precambrian Rift-related Transform System. Tectonics, **4**,497–511.

Swanberg C. A., Morgan P., Boulos F., 1983: Geothermal potential of Egypt. Tectonophysics, **96**, 77–94.

Tealeb A., Riad S., 1986. Regional tectonics of Sinai Peninsula interpreted from gravity and deep seismic data. In: Proceedings Fifth Annual Meeting of Egyptian Geophysical Society, Cairo, pp. 18–49.

Tramontini C., Davies D., 1969: A Seismic Refraction Survey in The Red Sea. Geophysical Journal International, **17**, 2, 225–241.

U.S. Geological Survey, 1963: Geological Survey research 1963; Short papers in geology and hydrology, Articles 1-59, Professional Paper 475-B.

Von Frese R. R. B., Hinze W. J., Sexton J. L., Braile L. W., 1982: Verifications of the crustal components in satellite magnetic data. Geophysical Research Letters, **9**, 293–295.

Wdowinski S., Bock Y., Baer G., Prawirodirdjo L., Bechor N., Naaman Knafo S., Forrai Y., Melzer Y., 2004: GPS measurements of current crustal movements along the Dead Sea Fault. Journal of Geophysical Research: Solid Earth, **109**, 1978–2012.

Woodside J. M., 1977: Tectonic elements and crust of the Eastern Mediterranean Sea. Marine Geophys. Res., **3**, 317–354.

Woodside J. M., 1976: Regional vertical tectonics in the Eastern Mediterranean Geophys. J. R. Astron. Soc., **47**, 493–514.

Youssef M. I., 1968: Structure pattern of Egypt and its interpretation. AAPG Bulletin, **52**(4), 601–614.

Zaghloul Z. M., Shaaban F. F., Yousef A. F., 1995: Subsurface Quaternary geothermal reservoir in the Nile Delta area. Journal of Environmental Sciences, **9**, 187–204.

Ziegler P. A., 1990: Geological Atlas of Western and Central Europe, Shell International Petroleum Mij. B. V., distributed by Geological Society, London, 2nd. Ed. Publishing House, Bath, 239 p.

Appendix I

If $g(x, y)$ is the gravity field then the horizontal gradient magnitude $HGM(x, y)$ is given by:

$$HGM(x,y) = \sqrt{\left(\frac{\partial g(x,y)}{\partial x}\right)^2 + \left(\frac{\partial g(x,y)}{\partial y}\right)^2}. \qquad \text{(A.1)}$$

The location of the horizontal gradient is computed by:

$$x_{\max} = \frac{-bd}{2a}\,, \tag{A.2}$$

where d is the grid interval and parameters a and b are defined as (Fig. 15):

$$a = \frac{1}{2}\left(HGM_{i-1,j} - 2HGM_{i,j} + HGM_{i+1,j}\right) \tag{A.3}$$

$$b = \frac{1}{2}\left(HGM_{i+1,j} - HGM_{i-1,j}\right)\,. \tag{A.4}$$

The horizontal gradient at $x_{\max}$ point is:

$$HGM_{\max} = ax_{\max}^2 + bx_{\max} + HGM_{i,j}\,. \tag{A.5}$$

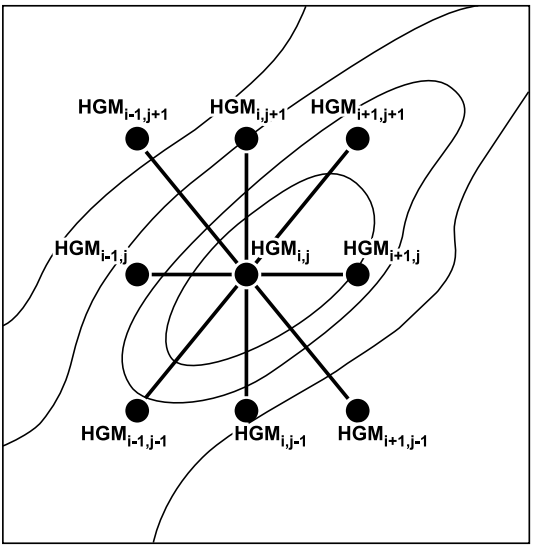

Fig. 15. Location of grid intersections used to test for a maximum near ($HGM_{i,j}$). Curved lines represent contours of horizontal gradient values of magnetic or gravity anomalies.